# Self-Assembly of 2D CdSe Semiconductor Nanoplatelets

by

Nina Alexandra Henke

Master thesis in Chemistry

submitted to the faculty of Chemistry, Pharmaceutical Sciences, Geosciences
(FB 09)
Johannes Gutenberg-University in Mainz

March 17th, 2020

1st reviewer: Prof. Dr. Katharina Landfester
2nd reviewer: Prof. Dr. Carsten Sönnichsen

# Selbstanordnung von 2D CdSe Halbleiter-Nanoplättchen

von

Nina Alexandra Henke

Masterarbeit in Chemie

vorgelegt dem Fachbereich Chemie, Pharmazie und Geowissenschaften (FB 09) der Johannes Gutenberg-Universität in Mainz

17.03.2020

1. Gutachter: Prof. Dr. Katharina Landfester
2. Gutachter: Prof. Dr. Carsten Sönnichsen

Eigenständigkeitserklärung

Masterarbeit im Studiengang Chemie
an der Johannes Gutenberg-Universität Mainz

Ich, Nina Alexandra Henke, Matrikelnummer 2715231, versichere, dass ich meine Masterarbeit selbstständig verfasst und keine anderen als die angegeben schriftlichen und elektronischen Quellen sowie andere Hilfsmittel benutzt habe. Alle Ausführungen, die anderen Schriften wörtlich oder sinngemäß entnommen wurden, habe ich kenntlich gemacht.

_____ _____

Ort, Datum Unterschrift

Nina Alexandra Henke
Johannes Gutenberg-Universität Mainz
Fachbereich Chemie, Pharmazie und Geowissenschaften (FB 09)
Duesbergweg 10-14
55128 Mainz
nhenke@students.uni-mainz.de

# Zusammenfassung

Energietransferprozesse finden sich im alltäglichen Leben wieder, beispielsweise bei der Photosynthese von Pflanzen oder der visuellen Wahrnehmung, sind gleichzeitig aber auch von großer Bedeutung für Solarzellen, Laser oder LEDs. Diese Anwendungen basieren auf funktionalen Materialien, welche verschiedene Formen von Energie ineinander umwandeln können, wie beispielsweise Halbleiternanokristalle, deren elektronische Bandlücke größen- und formabhängig verstellbar ist.[1] In den letzten Jahren wurde eine weitere Form von Nanokristallen entdeckt: quasi zweidimensionale Nanoplättchen (NPLs).[2] Die optische Eigenschaften von NPLs werden nur durch die einheitliche, atomar präzise Dicke der Kristalle bestimmt. CdSe NPLs zeichnen sich durch schmale Emissionsbanden, eine hohe Energietransfereffizienz, große Absorptionsquerschnitte und anisotrope Photolumineszenz aus und eignen sich daher als Bestandteil von optoelektronische Geräten. Für Anwendungen ist es jedoch notwendig, aus kolloidalen CdSe NPLs feste, geordnete Strukturen mit einer einheitlichen Orientierung der Nanoplättchen herzustellen. In Dispersion bilden Nanoplättchen, bedingt durch die anisotrope Form und daraus resultierenden, attraktiven van der Waals-Kräfte, bevorzugt stapelförmige Suprapartikel, in denen die lateralen Kristallfacetten zueinander hin ausgerichtet sind.[3] Auch die Herstellung von geordneten Filmen von CdSe-Nanoplättchen wurde im kleinen Maßstab untersucht.[4] Dabei kann der Anordnungsprozess von CdSe NPLs an einer flüssigen Grenzfläche entweder durch die gezielte Einstellung des Wechselwirkungspotentials zwischen NPLs oder durch kinetische Faktoren wie die Verdampfungsrate einer Dispersion von CdSe NPLs kontrolliert werden. Das Ziel dieser Masterarbeit besteht darin, eine zuverlässige Methode zur Herstellung von großflächigen Filmen mit einheitlicher CdSe-NPL-Orientierung zu entwickeln. Dafür wurden zunächst durch Selbstanordung der NPLs an einer flüssigen Grenzfläche erfolgreich Monolagen-Filme von CdSe-NPLs in ‚face-down'-Anordnung oder ‚edge-up'-Anordnung hergestellt und drei verschiedene Methoden zur Abscheidung der Filme auf feste Substrate evaluiert. Die erhaltenen Filme wurden mittels Transmissionselektronenmikroskopie in Bezug auf Größe, Struktur und Orientierung der Nanoplättchen charakterisiert. Es konnten Filme mit hoher Oberflächen-bedeckung und einer Größe von bis zu 2000 $\mu m^2$ hergestellt werden. Die Versuche zeigten auch, dass bei einer horizontalen Abscheidung der Filme die einheitliche Orientierung der CdSe-NPL erhalten bleibt, während eine vertikale Filmabscheidung zu einer gemischten Orientierung von NPLs in den Filmen führt. Mithilfe dieser Erkenntnisse konnten schließlich in zwei Schritten auch Doppellagen-Filme mit unterschiedlicher Anordnung der CdSe-NPLs hergestellt werden. Während der konsekutiven Abscheidung zweier Monolagen mit ‚face-down' orientierten Nanoplättchen wurde eine partielle Neuanordnung von NPLs in der oberen Schicht beobachtet, welche möglicherweise auf repulsive Kräfte zwischen Oberflächenliganden der CdSe-NPLs zurückzuführen ist. Zudem wurde die optimierte Methode zur Herstellung von CdSe-NPL-Filmen auf das Langmuir-Blodgett-Verfahren übertragen, was eine Beschichtung von größeren Substraten ermöglicht. Mithilfe des Langmuir-Blodgett-Verfahrens wurde das Kompressionsverhalten von Monolagen-Filmen untersucht. Dabei stellte sich heraus, dass ‚face-down' angeordnete Nanoplättchen durch langsame, horizontale Kompression irreversibel in eine ‚edge-up'-Position überführt werden können.

# Contents

# 1. Introduction

Energy transduction, the conversion of energy from one form to another, is at the centre of life and technology. In photosynthesis, plants convert light energy of photons into chemical energy for fueling the organisms' activities. Visual perception, the ability to detect and interpret our surrounding environment, is based on the transduction of visible light photons in our eyes into electrochemical potentials that are transmitted to the brain. In technology, optoelectronic devices like photovoltaic cells function by transducing light energy into electricity or vice versa, as is the case for light-emitting diodes and semiconductor lasers. All of these applications rely on functional materials that are capable of converting one form of energy to another. Nanomaterials in particular are suitable candidates due to their unique and tunable properties that result from quantum size effects. In semiconducting materials, the band-gap energy depends on the size and shape of particles and can therefore be adjusted during synthesis.[1] In recent years, quasi-2D nanoplatelets (NPLs) emerged as a novel type of semiconducting nanocrystals with distinct optical properties.[2] These highly anisotropic particles have an atomically precise thickness below the Bohr radius that defines their optical properties. As a result of uniform thickness, NPL ensembles exhibit narrow emission spectra, a major advantage compared to quantum dots (QDs). In addition, orientation-dependant features can result from the self-assembly of individual anisotropic nanocrystals into larger, ordered structures.[5,6] Thin films of CdSe NPLs exhibit an alignment of their emissive transition dipole moments in the NPL plane.[4] This is highly relevant as it enhances the electronic coupling between adjacent platelets and may thus improve the efficiency of NPL solar cells, LEDs and lasers.[7,8,9] Likewise, it is also expected to increase the radiative outcoupling-efficiency in displays or LED devices.[10] Therefore, a lot of research is being dedicated to controlling the three-dimensional long-range organization of self-assembled nanoplatelet structures. In colloidal solution, CdSe NPLs can be assembled into highly aligned stacks by addition of polar antisolvents or ligand exchange, thus tuning the interaction potential between nanoplatelets.[11,12] The formation of films was studied on a small scale in self-assembly experiments at the liquid interface.[4] Control over the orientation of CdSe NPLs was achieved by adjusting the interaction potential between nanoplatelets and subphase solvent, for example through addition of surfactant molecules like oleic acid.[4] Another straight-forward approach exploits kinetic effects caused by different solvent evaporation rates, demonstrating that the nanoplatelet configuration at the liquid interface can also be controlled by the choice of solvent. However, preserving the collective orientation of CdSe NPLs over larger areas is crucial for a future device integration. This project aims to develop an efficient procedure for the preparation of large nanoplatelet films with uniform coverage and good control over the nanoplatelet configuration. Monolayer and double-layer films of nanoplatelets in both face-down and edge-up orientations were prepared by self-assembly at the liquid interface and various methods were evaluated for the deposition of films onto solid substrates. Transmission electron microscopy served as the main characterization technique, allowing for the determination of size, structure and quality of films as well as the nanoplatelet orientation. Then, experiments were transferred to a Langmuir-Blodgett trough in order to study the self-assembly of CdSe NPLs at a larger scale. More importantly, this setup also offers an opportunity to study the compression behavior of CdSe NPL assemblies and to explore whether horizontal compression of monolayer films can evoke a change in NPL configuration.

# 2. Theoretical background

## 2.1 Colloidal nanocrystals

Nanocrystals are crystalline particles with dimensions in the range of 1-100 nm. Due to their small size, nanocrystals possess a significantly higher surface-to-volume ratio than bulk materials and as a result, their chemical behavior is more strongly dominated by the large surface area. While bulk materials have consistent properties, size-dependent properties are often observed at the nanoscale. An individual atom has a defined number of discrete energy states. When numerous atoms are combined to form a crystal lattice, their atomic orbitals overlap, split and form the same number of molecular orbitals, but each with a slightly different energy. Since the energy of adjacent states are nearly identical, they can be considered as a continuum or energy band of allowed electronic states. In semiconductors like CdSe, occupied states in the valence band and unoccupied states in the conduction band are separated by a fixed bandgap. The bandgap energy $E_g$ is a material constant within the range of a few eV, transitions between the bands due to thermal energy are mostly prevented at room temperature. However, the absorption of photons of UV-Vis light provides enough energy to excite an electron to the conduction band, thus leaving behind a hole in the valence band. The system can return to its ground state by radiative recombination of the electron-hole pair, emitting a photon in the process. Nanocrystals are made of a relatively small number of atoms and can be sorted in between single atoms and bulk materials, their electronic structure is comprised of mostly continuous bands with few discrete energy states near the band edges. The band gap of semiconductor nanocrystals changes as a function of the size of the particle. When the diameter of a semiconductor nanocrystal falls below the Bohr radius, a critical value which describes the average distance an electron in the conduction band and hole in the valence band, quantum confinement effects occur and lead to a quantization of the particles energy states.[13,14]

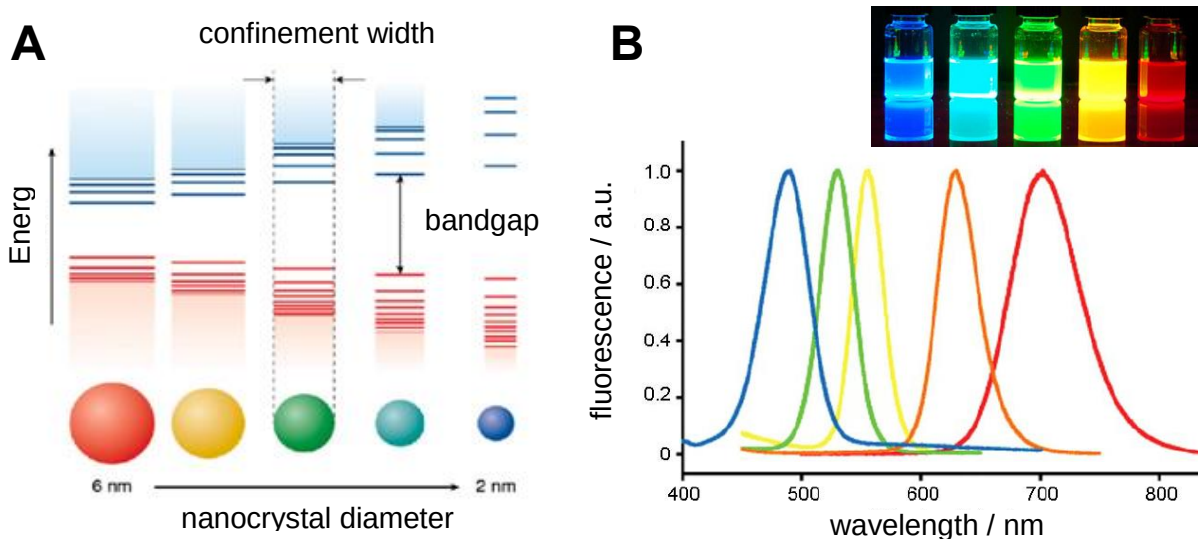


*Figure 1: Diagram of the electronic band structure in semiconductor nanocrystals (A).The semiconductor bandgap increases with decreasing nanocrystal size which leads to a blue-shift of the fluorescence wavelength (B). Adapted with permission from reference 14. Copyright 2010, American Chemical Society.*

As shown in Figure 1, a decrease in size reduces the number of atoms and splitting of their related states, thus resulting in a larger band gap between valence and conduction bands and a higher bandgap energy $E_g$.[15] The bandgap of CdSe nanocrystals, also referred to as quantum dots (QDs), can be shifted across the visbile light spectrum.

## 2.2 Quantum confinement and quasi-2D nanoplatelets

The properties of a confined semiconductor nanocrystal and its precise band-structure will further depend on its shape, that is, the number of dimensions over which the material is confined. Overall, there are three types of structures that can be produced from a confinement in either one, two or three dimensions. Quantum dots are confined in all three dimensions by their finite crystal lattice and can be compared to a particle in a box for which the box size is determined by the radius *r* of the QD and the energy of the particle, or electron, is proportional to $1/r^2$. The resulting discrete energy states appear as lines in the absorption spectrum and diagram in Figure 2.[16]

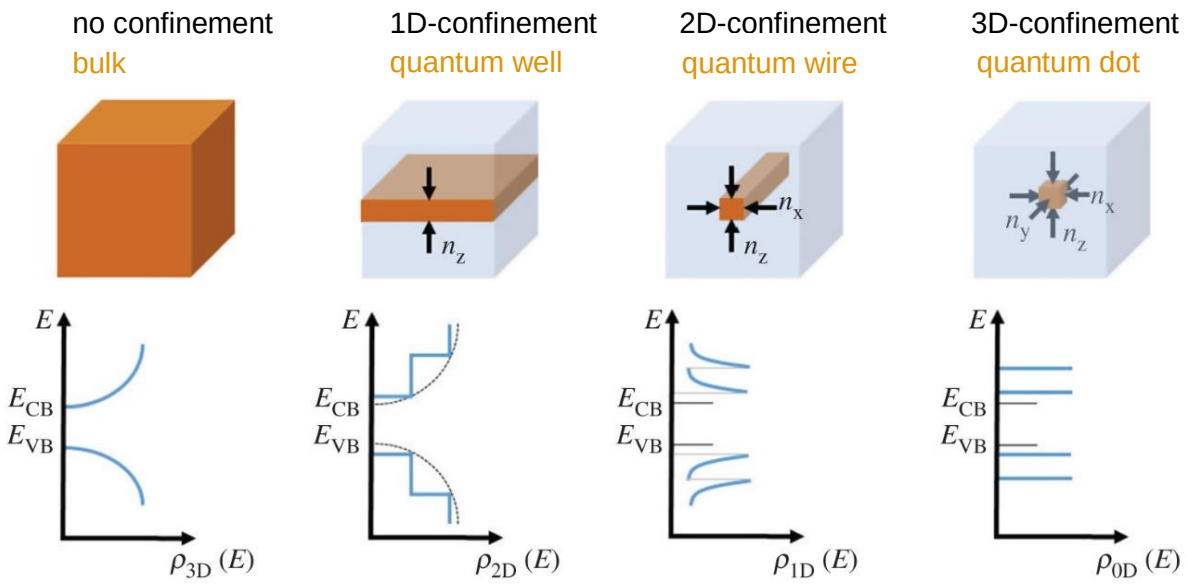


*Figure 2: Schematic representation of quantum dots, wires and wells. The density of states function for electrons in semiconductors is depicted for the bulk as well as for these types of confined structures. Adapted from reference 15. Copyright 2018, T. Edvinsson. http://creativecommons.org/licenses/by/4.0/.*

In quantum wires, the motion of electrons is confined in two dimensions whereas 2D-structures like thin films or nanoplatelets (NPLs) lead to a one-dimensional confinement, similar to a quantum well. The energy level $E_n$ only depend on the thickness *d* of the material and are given by the following equation 2.1, $m_{eh}$ is the effective mass of the electron-hole pair.

$$E_n = \frac{\hbar^2}{2\, m_{eh}} \cdot \frac{n^2 \pi^2}{d^2} \qquad (2.1)$$

Bulk semiconductors have a continuous absorption spectrum due to their continuous electronic band structure.

At the center of this work are semiconducting zincblende CdSe nanoplatelets, roughly square, quasi-2D crystals with a defined thickness in the range of 0.5 to 2 nm and lateral dimensions above the Bohr radius, typically between 10-30 nm. They are composed of alternating cadmium and selenium planes, whereby {001} cadmium planes terminate CdSe NPLs at all terminating facets.[17] On surfaces, cadmium atoms are bound to carboxylic acid X-type ligands[18] which serve to passivate the surface dangling bonds and stabilize nanoplatelets in dispersion.[19,20] An interesting feature of these materials is the ability to control their thickness in an atomically precise manner, so CdSe NPLs with a zinc blende lattice of exactly 3, 4 and 5 monolayers (ML) can be synthesized. Since a quantum confinement only occurs in one dimension, CdSe NPLs display distinct optical features which only depend on their thickness. Their absorption spectra in Figure 3 show characteristic bands of heavy-hole (HH) and light-hole (LH) electron transitions.[21] In emission spectra, the first exciton feature of 3 ML CdSe NPLs is found at a wavelength of  462 nm, 4 ML and 5 ML CdSe NPLs emit at 512 nm and 552 nm, respectively.

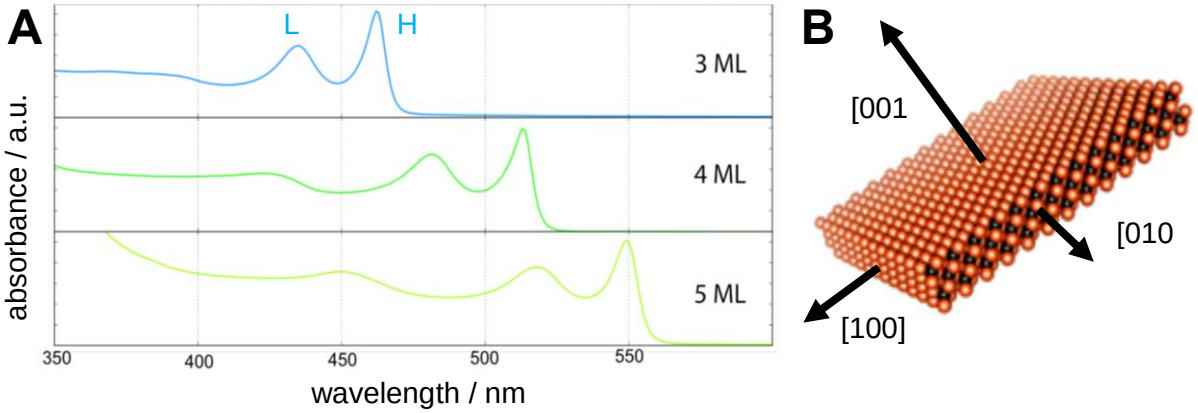


*Figure 3: UV-Vis absorbance spectra of colloidal CdSe NPLs with increasing thickness (A). Schematic model of an individual CdSe NPL with indication of relevant lattice directions (B). Adapted from reference 20. Copyright 2017, B. Abécassis.*

Due to the uniform thickness of CdSe NPLs ensembles, they exhibit spectrally pure fluorescence[22] with an exceptionally narrow line width around 10 nm.[23] Further features include enhanced energy transfer rates,[7] high energy transfer efficiency,[24] boosted optical gain[25] and large absorption cross-sections [26] and strongly anisotropic photoluminescence[27]. These properties make nanoplatelets suited for applications in optoelectronics, like light-emitting devices, solar cells or lasers. Here, device efficiency depends on electronic coupling between nanocrystals and thereby on the relative orientation of their transition dipole moments (TDM). Aligning transition dipole moments in isotropic materials poses a challenge and a mere stochastic distribution of TDM orientations results in a lower device efficiency. In anisotropic CdSe NPLs, transition dipole moments are intrinsically oriented in the plane of the platelet and ordered structures of NPLs naturally exhibit strongly directed emission.[4,27]

## 2.3 Colloidal forces between semiconducting CdSe nanoplatelets

In nanoscience, the self-assembly of nanocrystals is currently a topic of high interest. Using colloidal nanoparticles as building blocks, highly ordered and complex superstructures can be obtained.[28] Because of the way in which new collective effects often emerge from the formation of organized assemblies, many efforts are being dedicated to controlling the self-assembly process by tailoring the fundamental interactions between nanocrystals.[29] The most important contributions to attractive and repulsive forces between colloidal nanoplatelets are summarized in this section.
First, the existence of permanent dipoles in a nanocrystal affects interactions between colloidal particles through dipolar coupling. Indeed, a large dipolar moment was measured in CdSe QDs and highly anisotropic CdSe NPLs.[30,31] The interaction potential $V_{dipole}$ is given by equation 2.2 and depends on both the distance $r$ between dipole moments $\mu$ and their relative orientation to each other as is demonstrated in the scheme in Figure 4.

$$V_{dipole} = -\frac{\mu^2}{4\pi\varepsilon_0\varepsilon\, r^2} \cdot (2\, cos\theta_1 cos\theta_2 - sin\theta_1 sin\theta_2 cos\theta_3) \tag{2.2}$$

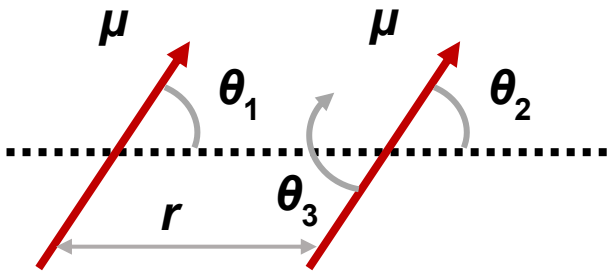


*Figure 4: Representation of relative dipole orientation by angles $\theta_1$, $\theta_2$ and $\theta_3$ and distance $r$.*

In nanoplatelets, maximum attractive interactions are achieved when the dipoles are in a parallel configuration since it enables the closest contact and thus the smallest distance $r$ between dipole moments located within the plane of NPLs.[21] Furthermore, attractive van der Waals forces, also referred to as London dispersion forces, contribute to the self-assembly of CdSe NPLs in a major way. Their origin lies in the interactions between induced dipoles in any given material. In general, van der Waals forces are considered short-ranged but the interaction potential $V_{vdW}$ is strongly dependant on the geometry of interacting particles.[32] For highly anisotropic nanoplatelets, the van der Waals potential $V_{vdW}$ per area unit scales with the distance $D$ between flat platelets by only $1/D^2$, as stated in equation 2.3 below.

$$V_{vdW} = -\frac{A}{12\pi D^2} \tag{2.3}$$

The Hamaker constant $A$ is a material constant, for a system of colloidal CdSe NPLs dispersed in a nonpolar solvent, it can be calculated from the individual Hamaker constants of CdSe and the respective solvent. Overall, attractive van der Waals forces decay much less rapidly for nanoplatelets compared to spherical particles which results in a significantly lower stability of CdSe NPLs in dispersion. Coulomb or electrostatic interactions are also known to have an important part in terms of colloidal stability and are therefore relevant to the self-assembly of nanocrystals.[33] The Debye length $\kappa^{-1}$ given by equation 2.4 describes the thickness of the electrochemical double layer which surrounds colloidal particles and contributes to stabilizing them in dispersion.

$$\kappa^{-1} = \sqrt{\frac{\varepsilon_0 \varepsilon k_B T}{e^2 \Sigma_i z_i^2 c_i}} \tag{2.4}$$

A thicker double layer is more effective in preventing the approach of two particles since the resulting repulsive forces between their equally charged surfaces are stronger. Surface charges may, for example, arise from incomplete ligand coverage so that the charges of surface atoms are not perfectly compensated. Whereas the Debye length is usually between 1 nm and 30 nm in water, depending on the charge $z_i$ and concentration $c_i$ of electrolytes, it can reach several µm in hexane or octane due to the low relative permittivity $\varepsilon$ of nonpolar solvents.[21] Charges from electrolytes are rare in these solvents, therefore any surface charges of particles only experience weak screening effects, thus acting over longer distances. Lastly, the impact of surfactant molecules bound to the surface of CdSe NPLs has to be considered. Myristate or oleate ligands are usually used in synthesis to disperse CdSe NPLs in organic solvents and provide colloidal stability to the dispersion. These X-type ligands[34] behave similarly to polymer chains in a good solvent. As soon as two nanoplatelets approach at distance that is smaller than twice the length of the surfactant layer, the alkyl chains of carboxylic acid units start to interpenetrate and compress, leading to repulsive forces between the particles. For a flat nanoplatelet covered with capping ligands, the free energy is comprised of two terms.[35,36] First, interpenetration of chains reduces configurational entropy because their mobility becomes limited. Second, the mixing of chains can be energetically favored or disfavored, depending on the quality or effectiveness of the solvent. If interactions between the surfactant layer and the solvent are stronger than between ligand chains, repulsive forces arise due to osmotic pressure and separate nanoplatelets from each other. The strength of ligand interactions also depends on the density of the surfactant layer and the ligand size, denser surfactant layers and ligands with a higher molecular weight will increase the repulsion between particles. In addition, recent theoretical calculations have taken the solvent molecules into account when determining the potential of two approaching nanoparticles. These calculations predict several potential wells at short distances that each correspond to a certain number of solvent molecules layers between the particles.[37,38]

## 2.4 Self-assembly of CdSe nanoplatelets

Colloidal CdSe NPLs demonstrate a strong tendency towards stacking due to their anisotropic shape and rather large lateral dimensions which result in strong van der Waals attractions between individual nanoplatelets.[3] The kinetics of this process highly depend on the size, concentration and ligand coverage of NPLs. While they can be stored in dispersion for days or even months, stacking will eventually occur as dispersed 2D-structures are not thermodynamically stable. In fact, face-to-face stacking of CdSe NPLs was confirmed by small-angle X-ray scattering (SAXS) measurements of nanoplatelet aggregates, SAXS patterns of stacked platelets exhibit sharp Bragg peaks at a separation which coincides with the center-to-center distance of NPLs within the stacks.[3,21] By addition of polar antisolvents like ethanol to CdSe NPL dispersions, the 1D-self-assembly can be drastically accelerated. ABÉCASSIS *et al*. even observed the formation of large needle-like supraparticles which are composed of up to $10^6$ individual nanoplatelets and show very strong in-plane polarization of emitted light.[11] Further collective properties that arise from stacking of CdSe NPLs include highly efficient homo-FRET as reported by GUZELTURK *et al.*[24] ROWLAND *et al.* also verified ultrafast energy transfer rates in the picosecond range for CdSe NPLs in a cofacial arrangement, which is significantly faster than nonradiative Auger-recombination, thereby making it a beneficial feature for applications in optoelectronic devices.[7]
The formation of thin films by solvent evaporation has been investigated as well. GAO *et al.* studied the self-assembly of CdSe NPLs at the diethylene glycol-hexane interface and controlled the configuration of nanoplatelets by addition of varying amounts of oleic acid to the subphase, thus effectively tuning the interaction potential between CdSe NPLs and diethylene glycole.[4]

In general, nanoplatelets can adopt the two orientations shown in Figure 5. If no or only a small amount of oleic acid is added to the subphase, the edge-up assembly is consistently observed whereas increasing the concentration of oleic acid in diethylene glycole yields face-down assemblies. Oleic acids acts as a surfactant, it reduces the interfacial tension between diethylene glycol and hexane while and thereby alters the interaction potential between the subphase and CdSe NPLs.

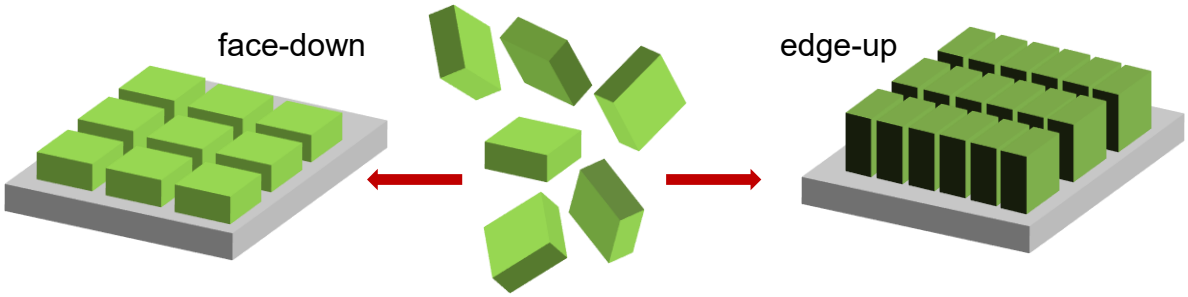


*Figure 5: Scheme of possible CdSe NPLs configurations in self-assembly experiments at the liquid interface, showing nanoplatelets in face-down orientation and edge-up orientation.*

An even more straight-forward and additive-free approach to obtaining collectively orientated CdSe NPLs assemblies was presented by the RIEDINGER group.[39] MOMPER *et al*. reported on exploiting solvent evaporation rates for kinetically controlling the self-assembly process of nanoplatelets at the acetonitrile-alkane interface.[39] Fast solvent evaporation prevents colloidal CdSe NPLs from forming stacks and yields the kinetically favored face-down configuration of nanoplatelets while slow solvent evaporation results in edge-up oriented nanoplatelets, the thermodynamically favored configuration. This mechanism was supported by experiments showing how the collective orientation of CdSe NPLs is indeed kinetically driven and can be controlled by parameters like choice of solvent, temperature as well as solvent vapor pressure in the atmosphere above the setup. Due to the facile experimental implementation, this method of self-assembly at the liquid interface will also be the basis for the preparation of CdSe NPL films in this project.

## 2.5 Preparation of thin films by Langmuir-Blodgett method

A controlled preparation of solid thin films is a fundamental step in integrating functional materials into devices. Common deposition methods are classified into two categories. Physical deposition can be achieved by sputtering, pulsed laser deposition or molecular beam epitaxy,[40] whereas chemical deposition includes methods like dip-coating, chemical vapor deposition and Langmuir-Blodgett method.[41,42,43] The experimental setup for thin film preparation by Langmuir-Blodgett method[44] is depicted in Figure 6.[45] A rectangular trough is filled with a polar solvent, the subphase, and particles dispersed in a volatile solvent are carefully applied to the liquid surface. After evaporation of the volatile solvent, two barriers on either side of the trough are compressed at a defined speed in order to adjust the packing density of particles at the liquid interface. During the compression process, changes in surface tension $\gamma$ are recorded by a probe wire or plate according to the Wilhelmy method.[32] Thus, a compression isotherm is obtained which depicts the surface pressure $\pi$ as a function of surface area $A$:

$$\pi = \gamma_0 - \gamma = RT\frac{c}{A} = RT\Gamma \qquad (2.5)$$

At low surface concentrations $\Gamma$, the particles carry out random motions at the subphase-air interface but the barrier movement slowly reduces the available surface area and thereby restricts the particles' motions, even further compression can evoke a behavior similar to phase transitions.

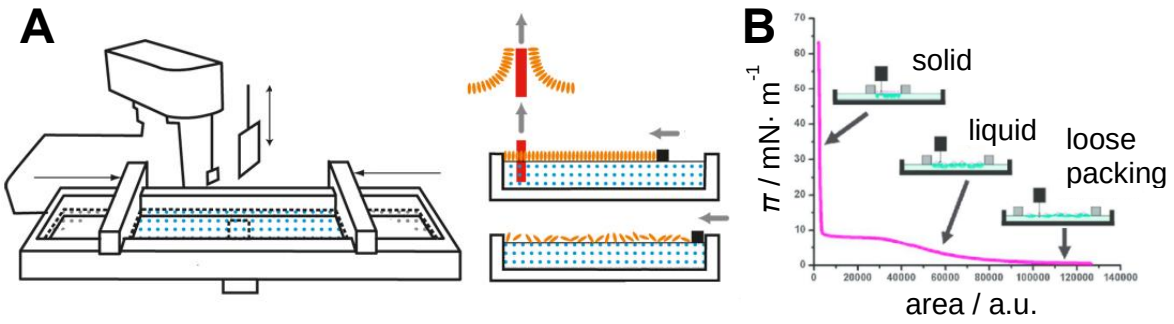


*Figure 6: Scheme of a Langmuir-Blodgett setup for thin film preparation and deposition (A). Compression isotherm of thin film preparation showing regimes with different packing behavior of particles at the interface (B). Adapted from reference 45. Copyright 2011, RusNano. http://creativecommons.org/licenses/by-sa/3.0/.*

In compression isotherms, different film states appear as sections with different slopes as can be seen from the example in Figure 6. Condensed monolayer films can be transferred onto various solid substrates by controlled vertical withdrawal of the solid substrate from the subphase. Applying horizontal pressure to a closely packed film causes the monolayer to collapse and multi-layered structures are formed. Then, the surface pressure either remains constant or decays abruptly if lateral compression was too fast for particle rearrangements. Langmuir-Blodgett thin films are typically composed of phospholipids, fatty acids or other amphiphilic molecules that readily assemble in a vertical manner at the liquid interface.[46] Nowadays, the method is also commonly used for preparing monolayers from nanoparticles[43,47] and KAUR *et al.* recently reported on the film preparation of inorganic phosphorene nanosheets, marking the first time of assembling 2D-materials by Langmuir-Blodgett method.[48] Following this, Langmuir-Blodgett method is deemed a promising technique for the preparation of thin mono- and multilayer films of quasi-2D CdSe NPLs.

# 3. Results and discussion

Earlier experiments in this group demonstrated that a collective orientation of CdSe NPLs can be achieved by kinetically controlling the self-assembly process at the liquid interface. Through the choice of volatile solvents with different vapor pressures, well-defined films of CdSe NPLs oriented in purely face-down or edge-up configuration were obtained by solvent evaporation of nanoplatelets dispersions.

The overall orientation of platelets in the monolayer film is mainly determined by the interactions between individual CdSe NPLs during the self-assembly process and the interaction potential between nanoplatelets and the subphase. First, it is important to consider that two-dimensional nanostructures like CdSe NPLs are typically less stable in dispersion than equally sized spherical nanocrystals. Due to their highly anisotropic shape, attractive van der Waals forces between the wide facets of CdSe nanoplatelets are stronger and extend over a long range, thereby promoting stacking of the colloidal particles in dispersion. Yet, to counteract these van der Waals attractions, the surface of CdSe NPLs is passivated with carboxylic X-type ligands during synthesis that serve to stabilize colloidal nanoplatelets by steric means. The negatively charged carboxylic groups of these ligands bind to positively charged cadmium ions of the CdSe NPLs and cap them off with non-polar alkyl chains, thus also rendering the whole NPL surface non-polar. Carboxylic acid ligands are generally classified as X-type ligands, meaning that they contribute one electron to the metal-ligand bond when using the neutral method of electron counting.[18] When two individual NPLs approach each other, at some point, the alkyl chains of said ligands begin to protrude into each other's rotational cones. This lowers their overall entropy and results in a repulsive force that keeps the nanoplatelets at distance and well-dispersed in the continuous phase. It should also be noted that the repulsive forces, and consequently, the effectiveness of steric stabilization increases with the density of surface ligands.

The interaction potential between CdSe NPLs and the subphase can be adjusted by the choice of subphase solvent. For example, GAO *et al.* added different amounts of oleic acid to a diethylene glycole subphase to alter the interaction potential of wide facets of NPLs with the diethylene glycole interface.[4] However, additives are not necessarily required to control the collective orientation of CdSe NPLs. Acetonitrile has a substantially lower polarity index compared to diethylene glycol, thus increasing the interaction potential between subphase and the lateral facets of CdSe NPLs and facilitating a face-down orientation of nanoplatelets. For this reason, acetonitrile was chosen as subphase solvent for self-assembly experiments in Teflon wells. Colloidal nanoplatelets dispersed in volatile alkane solvents were added on top of the subphase and the alkane solvent was left to evaporate. During this process, the NPL concentration increases steadily and, at a critical value of 4.3 µmol/L, anisotropic nanoplatelets start to agglomerate and form stacks. Now, the evaporation rate of the solvent determines the final orientation of nanoplatelets at the liquid interface. Upon fast evaporation, *i.e.* of hexane, CdSe NPLs are kinetically trapped in the face-down configuration whereas slower evaporation, *i.e.* of octane, leaves nanoplatelets with enough time to adopt the thermodynamically stable edge-up configuration.

Likewise, it is possible to control the collective orientation of CdSe NPLs in self-assembly experiments by varying the temperature or adjusting the solvent vapor pressure in the atmosphere above the setup. At low temperatures or high solvent vapor pressure, evaporation is decelerated and nanoplatelets assemble edge-up. In contrast, increasing the temperature or reducing the solvent vapor pressure accelerates solvent evaporation, resulting in face-down oriented NPLs. However, varying the solvent of CdSe NPL dispersions to assemble nanoplatelets either purely face-down or purely edge-up represents the easiest approach to controlling solvent evaporation. Focusing on the quality of obtained films in terms of size and surface coverage, this project aimed to develop a reliable procedure for the preparation of large, mostly even and coherent films of CdSe NPLs while still maintaining control over the collective configuration of nanoplatelets. This is a critical step towards establishing quasi-2D nanostructures such as CdSe NPLs as suitable materials for applications in the field of optoelectronics. Therefore, various experimental setups and methods of film deposition were developed and tested. An overview of methods I, II and III is depicted in Figure 7, along with photographs of a Teflon well used for self-assembly experiments at the liquid interface.

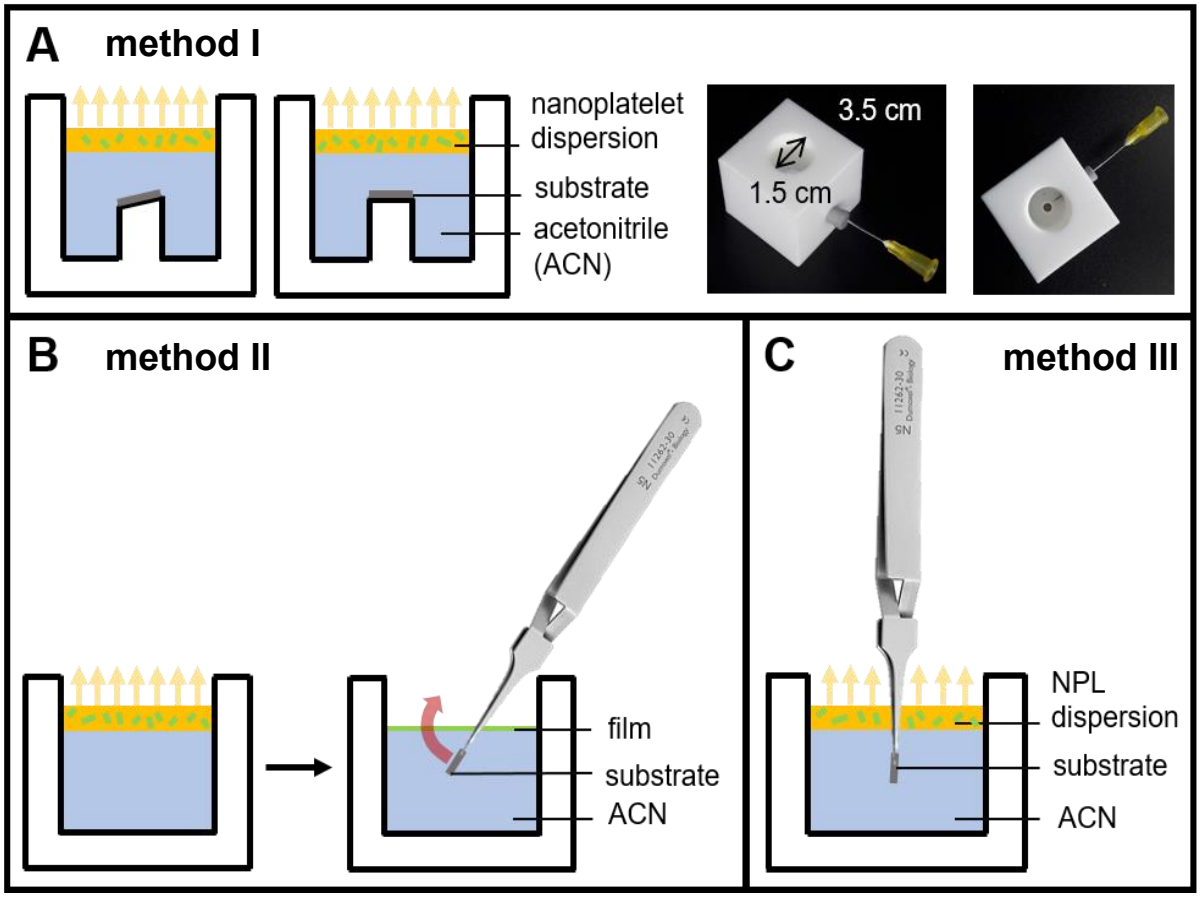


*Figure 7: Overview on evaluated methods for deposition of CdSe NPL films onto solid substrates. The substrate is placed on a level or sloped platform in method I (A), immersed in the subphase after film formation and lifted in method II (B) or vertically dipped in the Teflon well in method III (C). Photographs of a Teflon well used for self-assembly experiments are included.*

In method I (Figure 7A), self-assembly experiments of CdSe NPLs were carried out in 3.5 cm x 3.5 cm x 3.0 cm Teflon well according to a procedure described by GAO *et al.*[4] and modified by the MOMPER *et al.*[39] Acetonitrile was used as a subphase for the self-assembly at the liquid interface and 4 ML CdSe NPLs dispersed in either hexane or octane were added on top after the substrate, a carbon-coated copper TEM grid, was placed on a small cylindrical platform in the center of the Teflon well. After evaporation of the alkane solvent, the acetonitrile subphase is slowly drained *via* a syringe near the bottom of the well, thereby lowering and depositing the formed film of CdSe NPLs at the interface onto the solid substrate. The slope of the cylindrical platform was also varied in self-assembly experiments. Starting with a level platform of 0° tilt angle, it was later replaced with a similar platforms sloped at an angle of 10° and 20° to examine if a smoother transfer of the films from interface to solid substrate, and thus a more uniform surface deposition, can be achieved with a modified setup.

In method II (Figure 7B), the platform is removed and colloidal CdSe NPLs are added on top of the acetonitrile phase without first placing the substrate in the Teflon well. This approach was tested to improve on the size of coherent nanoplatelet monolayer films since the draining of the acetonitrile subphase can cause tearing of films during deposition. Method II does not require the draining of the acetonitrile subphase in order to transfer the film at the liquid interface onto the substrate. Instead, the substrate is coated by immersing it in the Teflon well after the self-assembly of CdSe NPLs and complete evaporation of the alkane solvent, followed by upward lifting. If persecuted carefully, this method should allow for a more precise placement of the floating film on the substrate surface.

Another third method was tested for the self-assembly of CdSe NPLs at the liquid interface which bears similarities with dip-coating, a film deposition technique that is commonly used in nanomaterial engineering for the fabrication of thin film coatings.[49] In method III (Figure 7C), the substrate is held by tweezers attached to a stand and is immersed in the acetonitrile subphase. Then, 4 ML CdSe NPLs dispersed in hexane or octane are added to the interface and the Teflon well is kept undisturbed, letting the alkane solvent evaporate. Compared to method I and method II, the Teflon well could not be covered in method III as a glass dish would interfere with the experimental setup. After complete solvent evaporation, the film is transferred onto the substrate by slowly draining the acetonitrile subphase *via* the syringe. The vertical manner in which the monolayer film of CdSe NPLs is transferred onto a solid substrate also resembles the deposition by Langmuir-Blodgett method.

These methods were compared and evaluated according to criteria such as control over nanoplatelet configuration, size and quality of obtained films as well as the feasibility and reliability of each presented method. Later, self-assembly experiments were conducted in a Langmuir-Blodgett trough, an established setup for the fabrication and homogeneous deposition of monolayer thin films onto solid substrates that allows for studying self-assembly of CdSe NPLs on a larger scale.

## 3.1 Synthesis and characterization of CdSe nanoplatelets

First, colloidal 4 ML CdSe nanoplatelets were synthesized from a $Cd(myristate)_2$ precursor, $Cd(acetate)_2$ and selenium powder as described in the experimental section. In order to determine their size, shape and overall size distribution, they were analyzed by transmission electron microscopy (TEM). Representative examples of as-synthesized CdSe nanoplatelets dispersed in hexane are shown in Figure 8: TEM images of CdSe NPLs both lying down flat on the substrate (A) and forming ordered stacks (B). Histogram and distribution function of the edge length of 4 ML CdSe NPLs.Figure 8. The nanoplatelets can be seen both lying flat on the substrate (Figure 8A) and forming stacks while standing on the edge (Figure 8B). Higher magnifications confirm that the platelets are roughly square-shaped with relatively sharp edges. The average edge length was derived from measuring 4 monolayer (ML) CdSe nanoplatelets with the software *ImageJ* and amounts to 11.1±0.1 nm (Figure 8C). The tendency to form ordered stacks is a result of attractive Van der Waals forces between colloidal CdSe nanoplatelets; it is especially favored if NPLs are uniformly shaped and show only small deviations in size as can be observed for the 4 ML CdSe NPLs synthesized in this project.

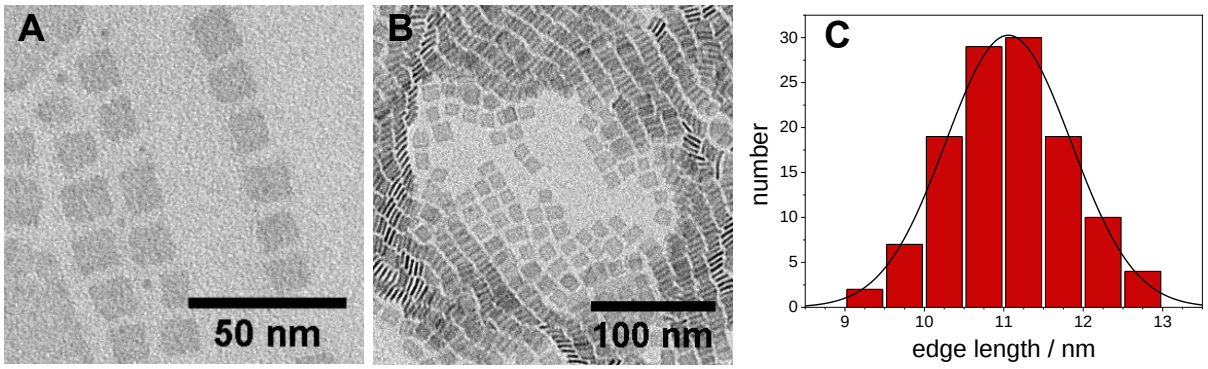


*Figure 8: TEM images of CdSe NPLs both lying down flat on the substrate (A) and forming ordered stacks (B). Histogram and distribution function of the edge length of 4 ML CdSe NPLs.*

Figure 9 depicts the UV-VIS absorbance and fluorescence spectra of the as-synthesized reaction mix of CdSe nanoplatelets (Figure 9A) and purified 4 ML CdSe nanoplatelets dispersed in hexane. The fluorescence spectrum of the crude reaction mixture displays characteristic peaks of 3 ML CdSe NPLs at 463 nm, 4 ML CdSe NPLs at 513 nm and 5 ML CdSe NPLs at 547 nm. A broad signal at 550-670 nm also points to the existence of few CdSe QDs in the reaction mix. CdSe NPLs with a thickness of 3 ML and 4 ML were separated from 5 ML CdSe NPLs and QDs by centrifugation and were re-dispersed in hexane. Within 1-2 weeks of storage at room temperature, 3 ML CdSe NPLs precipitate due to their lower colloidal stability and can be easily removed by another centrifugation step. The stepwise growth mechanism of quasi-2D CdSe NPLs described by Ott *et al*.[50] predicts that 3 ML CdSe NPLs have larger lateral dimensions than 4 ML and 5 ML CdSe NPLs obtained from the same synthesis. This is indeed confirmed by TEM images of non-purified samples.

Furthermore, 4 ML CdSe NPLs were precipitated in 1:1 methyl acetate and hexane and subsequently re-dispersed in hexane to remove remaining traces of 1-octadecene and free oleic acid from the dispersion. This is a necessary step in the sample preparation for self-assembly experiments since it was shown that traces of both chemicals can influence the configuration of CdSe NPLs during self-assembly at the liquid interface.[4]

As can be seen from Figure 9, the purified 4 ML CdSe nanoplatelets show a single characteristic, narrow fluorescence band at 513 nm (Figure 9B) attributed to the band edge recombination of an electron in the conduction band and a hole in the valence band of the platelet. The line broadening of this band is merely a result of thermal energy variations between NPLs.[23] The absorption spectrum exhibits a broader band at 481 nm and another narrow band of higher intensity at 513 nm (Figure 9B). This is in agreement with theoretical predictions and can be easily interpreted by comparing the electronic band structure of quasi-2D nanoplatelets to the model of a 1D-potential quantum well. These two peaks correspond to the heavy hole-electron and light-hole electron transitions. It should also be noted that since the maxima of absorption and emission coincide almost exactly at a wavelength of 513 nm, the respective spectra of 4 ML CdSe NPLs have an especially large overlap. This property contributes to an effective energy transfer between nanoplatelets, thus making them suitable materials for many optoelectronic applications.

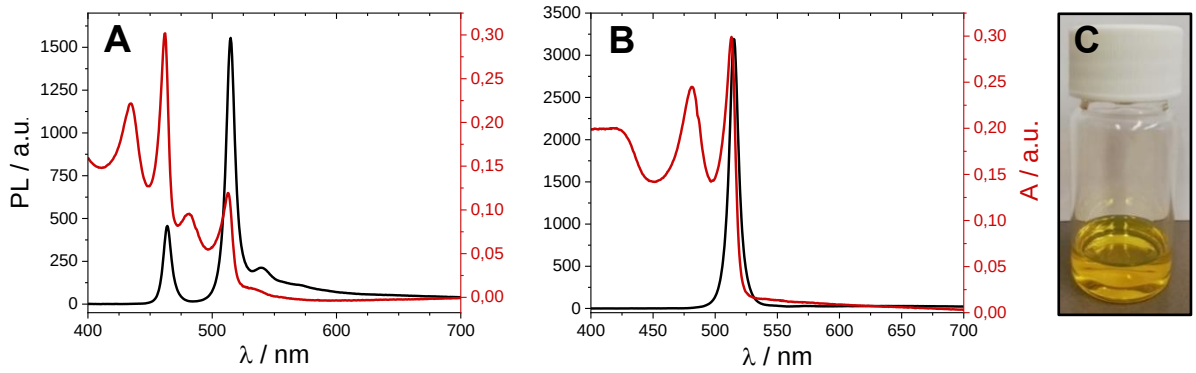


*Figure 9: UV-Vis absorbance and fluorescence spectra of the reaction mixture containing 3 ML, 4 ML, 5 ML CdSe NPLs and CdSe QDs (A) and respective spectra of the purified 4 ML CdSe NPLs (B). Colloidal 4 ML CdSe NPLs dispersed in hexane (C).*

Figure 9 also shows a bright yellow dispersion of 4 ML CdSe NPLs in hexane, the synthesis and following purification process yields stock dispersions with 4 ML CdSe NPL concentrations in the range of $10^{-7}$ - $10^{-6}$ mol/L.

In addition to characterization by size, shape and optical properties, the ligand coverage of 4 ML CdSe NPLs was determined by thermal analysis. Thermogravimetric analysis (TGA) can provide information about the number of ligands on the NPL surface by detecting the weight loss caused by complete decomposition of organic myristate ligands. This is relevant to self-assembly experiments because the density of the surfactant shell has a major influence on repulsive forces between colloidal CdSe NPLs and can thus alter the kinetics of the self-assembly process.[21] The results of thermogravimetric analysis of a purified 4 ML CdSe NPL solid are plotted in Figure 10.

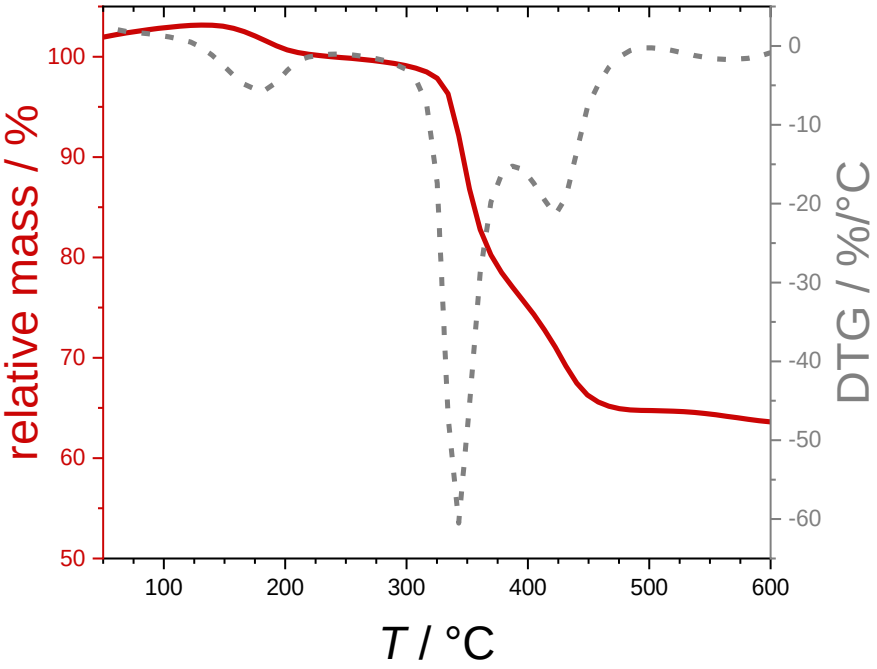


*Figure 10: Thermogravimetric analysis of precipitated 4 ML CdSe NPLs in the range of 50-900 °C at a heating rate of 10 °C/min. Relative mass (red line) and the first derivative of the relative mass (dotted grey line) are plotted against temperature.*

In the temperature range of 50 °C - 900 °C, a total weight loss of 45 % was observed, the largest decrease of mass takes place at around 350 °C. While the CdSe lattice is of NPLs is stable at these temperatures, cadmium myristate decomposes above 234 °C.[51] Therefore, the weight loss between 320 °C and 400 °C can be attributed to the decomposition of myristate ligands. The number of myristate molecules per nanoplatelet $N_{TGA}$ was calculated by equation (3.1) from the absolute mass $m_0$ before decomposition and the absolute weight loss $\Delta m$ in the relevant temperature range. The density of a zincblende CdSe lattice $\rho$[52] and the molar mass of myristic acid $M$ were taken from literature, the average volume of an individual CdSe NPL was determined from its dimensions:

$$N_{TGA} = \frac{\Delta m \cdot V \cdot \rho}{m_0 \cdot M} = \frac{3.6932\ \text{mg} \cdot 147.852\ \text{nm}^3 \cdot 5.655\ \text{g/cm}^3}{10.5512\ \text{mg} \cdot 228.371\ \text{g/mol}} = 1187 \qquad (3.1)$$

To make an assessment of this value, further calculations were performed to determine a theoretical number of myristate ligands $N_i$ that can be placed on the surface of a CdSe NPL with dimensions of 11.1 nm x 11.1 nm x 1.2 nm. It is possible to estimate $N_i$ by considering the entire surface of a CdSe nanoplatelet, $O_{NPL}$ = 299.7 nm$^2$, compared to the required area of the carboxylic group of a myristate ligand binding to the NPL, $A_{COO^-}$ = 0.220 nm$^2$. The latter value was calculated with trigonometric equations from C-O and C=O bond lengths and the shape of the required area was assumed to be spherical. This way, a value of $N_i^1$ = 1362 is obtained.

Alternatively, the surface of a CdSe nanoplatelet can be compared to the area of one side of a zincblende CdSe unit cell $A_{uc}$ = 0.370 nm$^2$. Given the face-centered cubic lattice of cations, this area includes two cadmium atoms. So, assuming that every cadmium atom on the surface is bound to one myristate molecule, the theoretical number of ligands amounts to $N_i^2$ = 1620. Looking at both theoretical values, the value obtained from TGA data lies within a realistic range and yields a ligand coverage of 73-87% or 4 ligands per nm$^2$. This is also in good agreement with literature in which values of 3-4 ligands per nm$^2$ were determined by $^1$H-NMR spectroscopy for oleic acid-capped CdSe QDs.[53] The calculations of $N_i$ do not consider the volume and flexibility of alkyl chains which can account for a higher space requirement per ligand and thus a ligand coverage lower than 100%. It should also be noted that oleic acid, a common capping ligand for CdSe nanoparticles, was added during the synthesis of CdSe NPLs to terminate the growth process. Therefore, myristate ligands could have been partially substituted by oleate ligands, resulting in a two-component ligand shell around nanoplatelets which complicates the evaluation of TGA data. Oleate ligands possess a double bond and a longer alkyl chain which should strengthen repulsive forces between colloidal NPLs compared to myristate ligands. However, no characteristic peak of the double bond in oleic acid was found in $^1$H-NMR spectra of CdSe NPLs depicted in Appendix 1. In summary, thermal analysis revealed a relatively high ligand coverage, suggesting a dense ligand shell surrounding the nanoplatelets. Therefore, repulsive forces induced by interpenetration of capping ligands have to be regarded as an important influence on the self-assembly of CdSe NPLs.

## 3.2 Preparation of CdSe nanoplatelet monolayer films by method I

After a successful synthesis and characterization of 4 ML CdSe NPLs, self-assembly experiments were carried out in Teflon wells. The film formation and deposition process was studied at a small scale to evaluate different experimental setups and methods for the preparation of large, coherent films of collectively oriented nanoplatelets. The TEM images in Figure 11 depict monolayer films which were prepared from hexane dispersions of 4 ML CdSe NPLs by method I. The substrate, a TEM grid, was placed on a level platform with 0° tilt angle. At high magnifications, the almost purely face-down orientation is clearly visible (Figure 11A), thereby demonstrating that good control over the orientation of CdSe NPLs is maintained by this method. Only very few nanoplatelets are found in the edge-up configuration and the film thickness is fairly consistent as well (Figure 11B). Lower magnifications show the overall size and shape of monolayer films. In some cases, areas of up to 10 µm x 10 µm are entirely covered with nanoplatelets (Figure 11C) but in most other regions of the substrate, the films are unevenly shaped and patchy (Figure 11D). Since CdSe NPLs are only 4 monolayers or 1.2 nm thin, it is to be expected that interactions between the narrow facets are weaker than between the wide facets and also depend more strongly on the relative orientation, that is, the angle between the planes of two individual nanoplatelets. So lower cohesions forces between CdSe NPLs in the plane of the monolayer could lead to patchy films. However, increasing the surface concentration of CdSe NPLs in self-assembly experiments should reduce free space between nanoplatelets at the interface and thereby improve the quality of monolayer films.

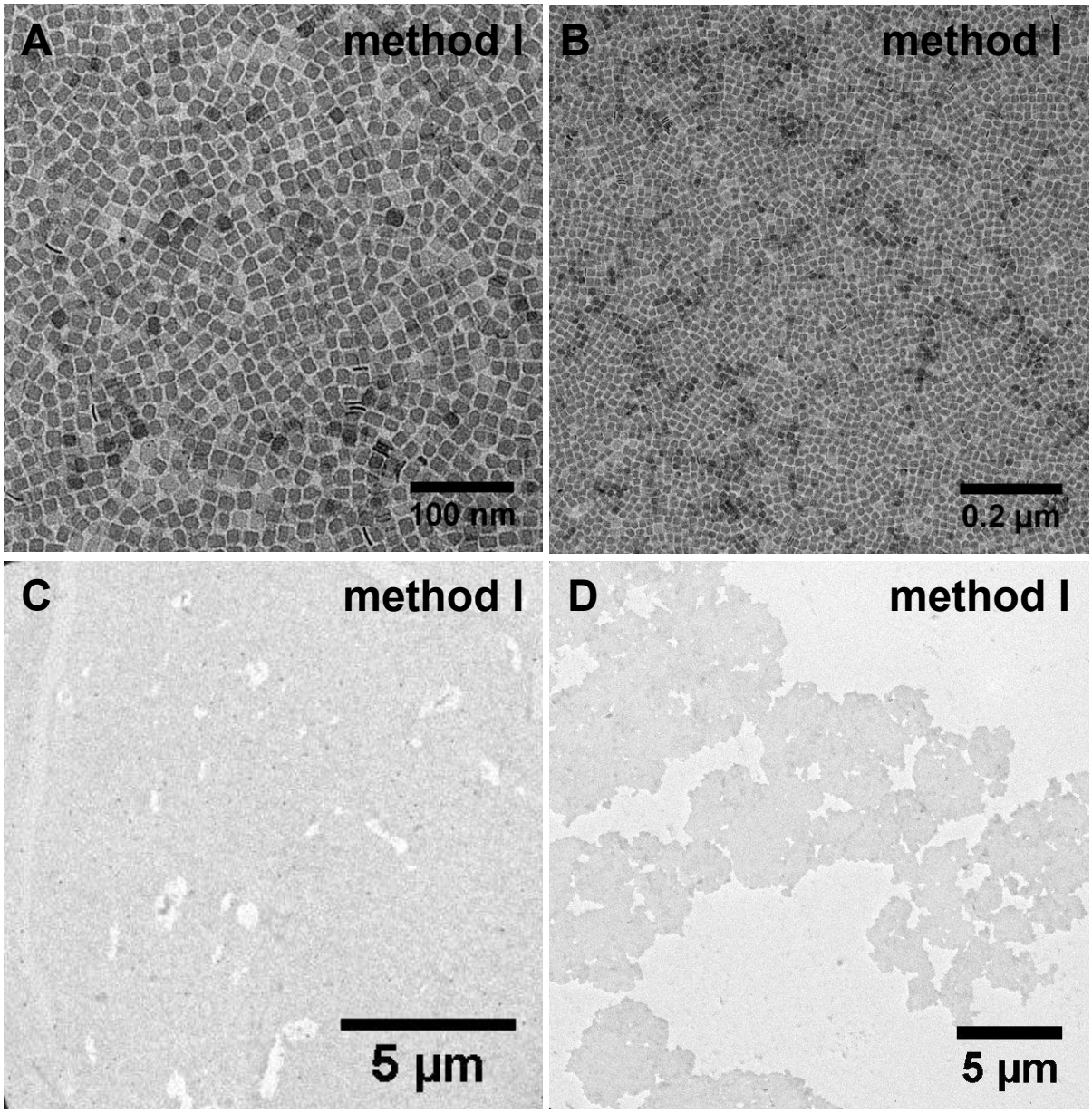


*Figure 11: TEM images of face-down monolayer films prepared by **method I** from 4 ML CdSe NPLs dispersed in hexane. **Tilt angle of platform is 0°**. Images were recorded at different magnifications.*

Figure 12 shows TEM images of monolayer films which were prepared from octane dispersions of 4 ML CdSe NPLs by method I, again using a level platform for positioning of the substrate. All CdSe NPLs are oriented in the thermodynamically favored edge-up configuration and form stacks with an average length of around 100 nm (Figure 12A). Some nanoplatelets within the stacks are also slightly tilted (Figure 12B). The stack length is most likely temperature dependent and should increase with lower temperatures since the evaporation rate of the solvent decreases, giving the stacks more time to arrange and thereby enabling the colloidal CdSe NPLs to form larger supramolecular structures. Here, stacks do not show a clear direction of arrangement in these TEM images (Figure 12C) but regions with higher degree of order are visible where stacks are well aligned next to each other (Figure 12B).

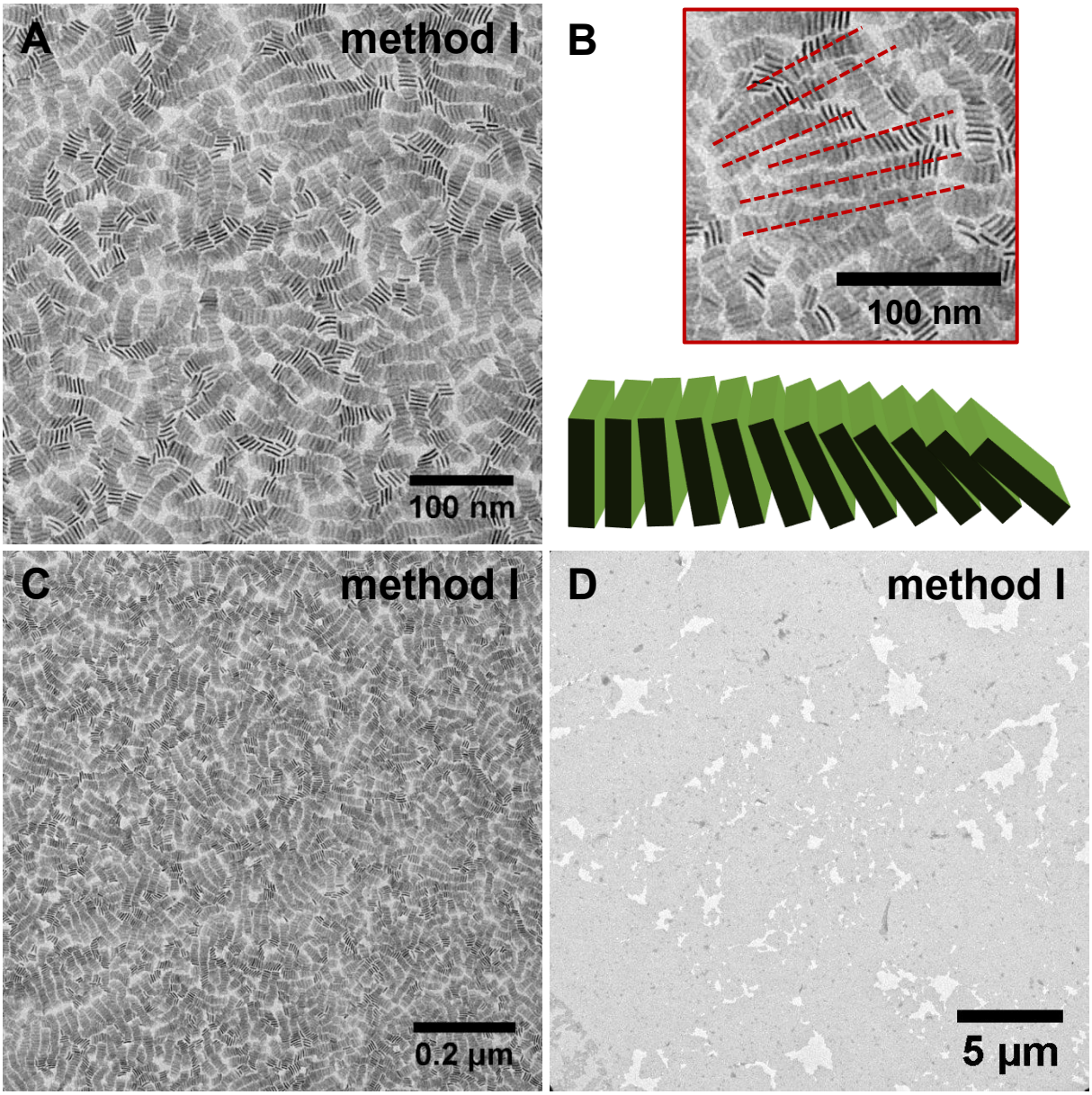


*Figure 12: TEM images of edge-up monolayer films prepared by **method I** from 4 ML CdSe NPLs dispersed in octane (A, C, D). Aligned nanoplatelet stacks and scheme of stacking (B). **Tilt angle of platform is 0°.***

In earlier experiments, angle-dependent photoluminescence spectroscopy on CdSe NPL monolayer films prepared at 5 °C demonstrated a preferential, long-range order of edge-up oriented CdSe NPL stacks that is maintained over a range of at least 5 $mm^2$.[39] It should be noted that the monolayer films of CdSe NPLs oriented edge-up are larger in size and more even compared to films with face-down oriented nanoplatelets, thus a better surface coverage of the substrate can be achieved (Figure 12D).

Still, tearing of the fluorescent CdSe NPL monolayer films was commonly observed under UV light when draining the subphase, resulting in incomplete transfer of the film onto the solid substrate. Although these macroscopic cracks do not sufficiently explain the patchy structure of face-down monolayer films, the experimental setup was slightly modified by replacing the level platform with a similar platform sloped at an angle of 10° or 20°.

This could help to guarantee a smoother transfer of films from interface to solid substrate and reduce tearing of films. TEM images of face-down monolayer films that were obtained by using the modified Teflon well setup are shown in Figure 13. In comparison with TEM images of monolayer films obtained with a standard setup of method I, no significant differences were found in terms of overall surface coverage and film structure. In both cases, few segments larger than 10 µm x 10 µm of the substrate were completely covered with nanoplatelets.

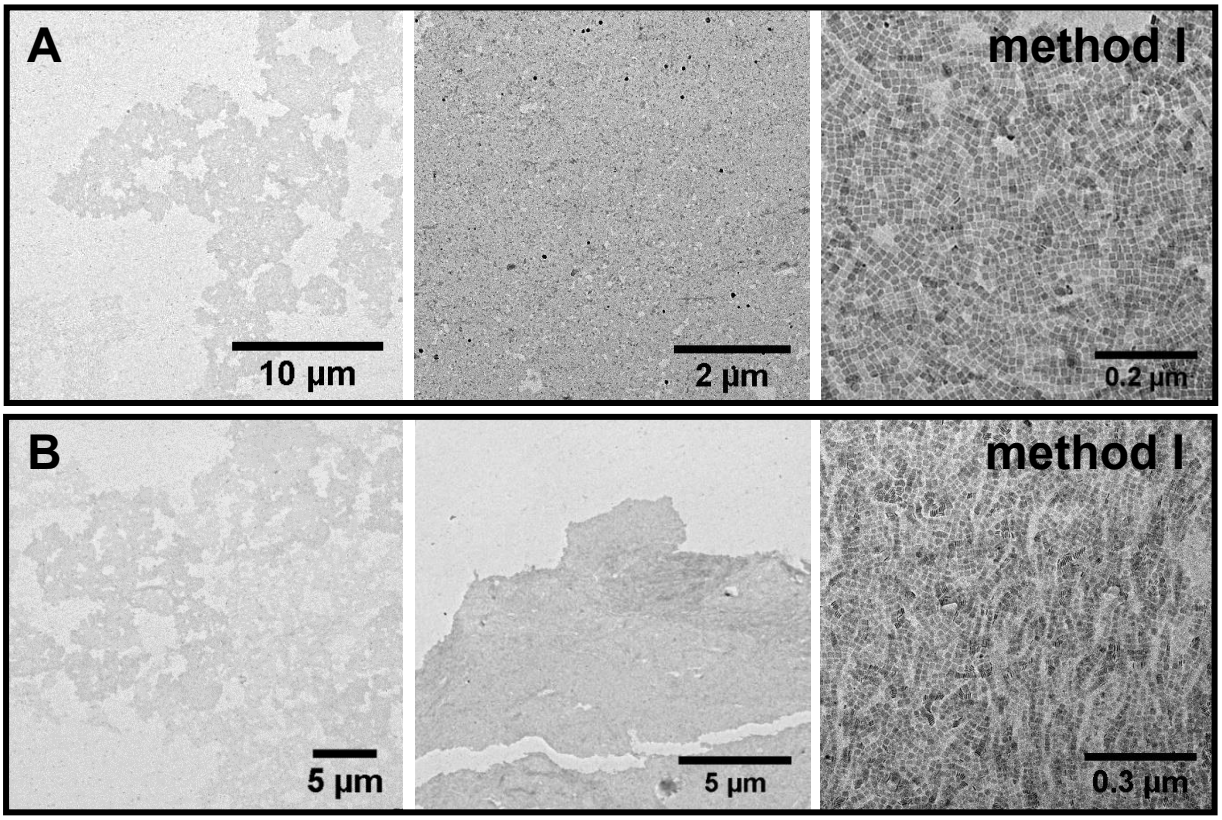


*Figure 13: TEM images of face-down monolayer films prepared by **method I** from 4 ML CdSe NPLs dispersed in hexane. **Tilt angle of platform is 10°** (A) **and 20°** (B). Images were recorded at different magnifications.*

Again, monolayer films are patchy for the most part. Still, control over the collective orientation of NPLs is maintained as well, as can be seen from higher magnification images. At a platform slope of 20°, nanoplatelets are arranged in flowing patterns (Figure 13B) which might be caused by a downward flow of acetonitrile along the substrate surface during the draining process. Also, film deposition by method I is more readily feasible with a standard setup including a level platform as the substrate placement proves more difficult on a sloped platform. Overall, this method allows for good control over NPL configuration in monolayer films, but modifications of the experimental procedure are necessary to improve on the film size and surface coverage of the substrate, especially in case of face-down oriented nanoplatelets. It should be noted that the differences in film structure between edge-up and face-down oriented nanoplatelets can also just be a result of different drying dynamics. The structures formed on surfaces or interfaces from the drying of liquid films or droplets containing colloidal nanoparticles can vary significantly, depending on the nature of suspended particles and interface, the solvent, vapor pressure and surrounding airflow.[54]

Within the scope of this project, a stronger focus is placed on the preparation of good quality films with CdSe NPLs in the face-down configuration since large films with edge-up oriented nanoplatelets are more readily formed in general.

## 3.3 Preparation of CdSe nanoplatelet monolayer films by method II

As film tearing was often observed during the draining process of method I and mostly smaller coherent films were transferred to the substrate, a second method of film deposition was evaluated that did not require a draining of the subphase and allowed for a precise placement of floating films onto the substrate.

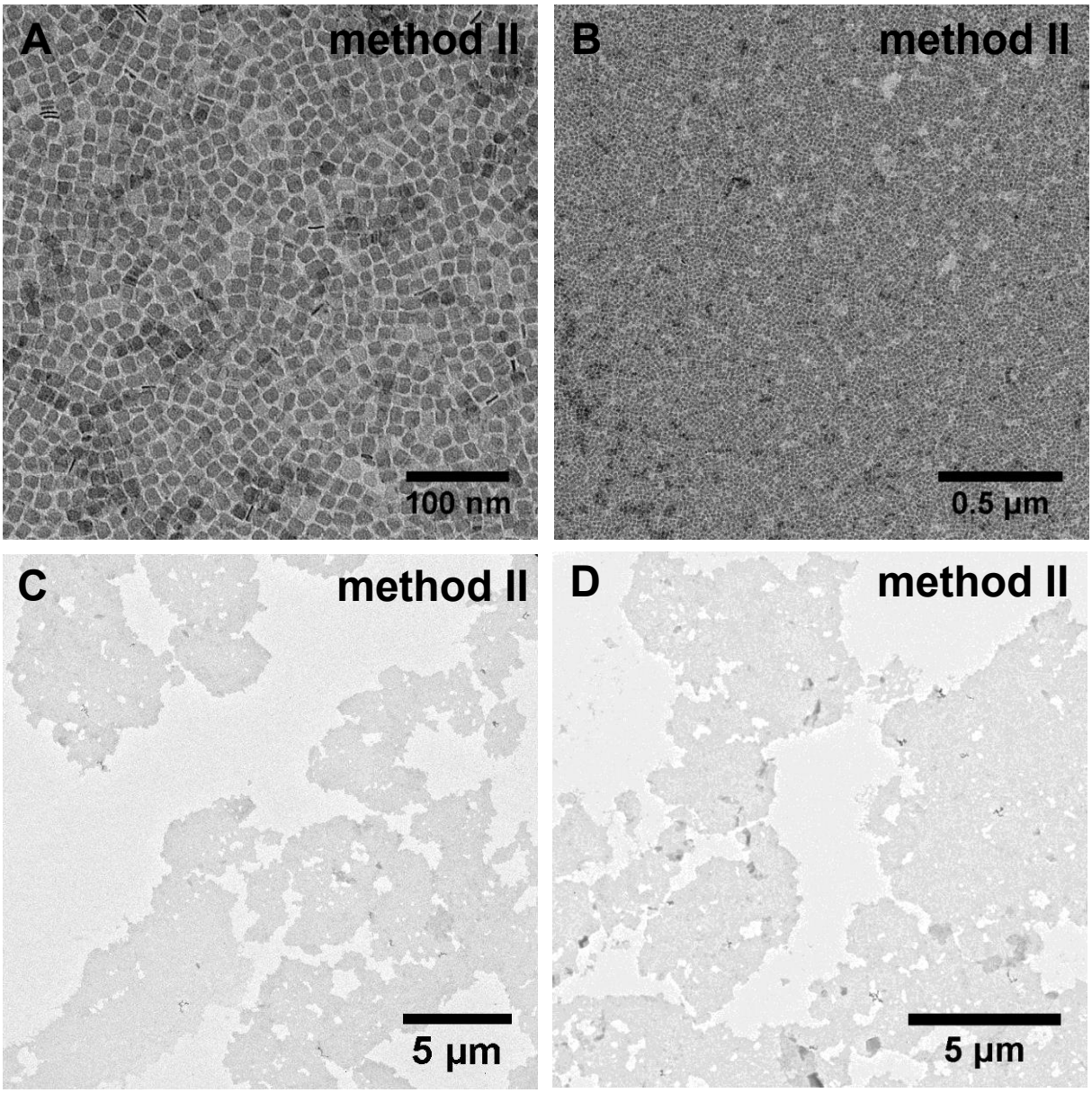


*Figure 14: TEM images of face-down monolayer films prepared by **method II** from 4 ML CdSe NPLs dispersed in hexane. Images were recorded at different magnifications.*

TEM images of face-down monolayer films prepared by method II are depicted in Figure 14. High magnifications confirm that CdSe NPLs (Figure 14A) adopted a face-down orientation as is to be expected for nanoplatelets dispersed in hexane. The film thickness is fairly consistent (Figure 14B) but no obvious improvements were achieved with this method in terms of size and shape. Although there was indeed no tearing of fluorescent films observed under UV light, the films are irregularly shaped, with coherent parts in a size range of 25 $\mu m^2$ to 50 $\mu m^2$ (Figure 14C-D). This confirms earlier assumptions that the patchy structure of face-down monolayer films is not a result of macroscopic tears. Instead, this issue could arise from too low CdSe NPL concentrations at the liquid interface which will be further discussed and verified in the next section.

## 3.4 Improving the surface coverage of face-down monolayer films

Both method I and method II yield monolayer films with almost pure face-down orientation of NPLs when prepared from dispersions in hexane and edge-up orientation of NPLs when prepared from dispersions in octane.

Experiments of CdSe NPL self-assembly by solvent evaporation are straight-forward to implement but TEM images show that, with current experimental parameters, they produce patchy films of face-down oriented platelets. Considering the area required by an individual CdSe NPL capped with myristate ligands in the face-down configuration $A_{NPL}$ and the total interface area in the Teflon well $A_{well}$, the theoretical surface coverage for a monolayer film using a CdSe NPL dispersion of a given volume $V$ and concentration $c$ is calculated according to equation 3.2 below. So far, a volume of $V$ = 50 µL CdSe NPLs dispersed in hexane were added to the Teflon well in each experiment, the concentration of nanoplatelets was determined by UV-Vis absorption spectroscopy and amounts to $c_{NPL} = 2.98 \cdot 10^{-8}$ mol/L.

$$x_{\%} = \frac{c \cdot V \cdot A_{NPL} \cdot N_A}{A_{well}} \cdot 100\% \qquad (3.2)$$

The average edge length of square 4 ML CdSe NPLs was determined in section 3.1 from TEM images and is 11.1 ± 0.2 nm. The distance between NPLs in face-down monolayer films was also determined manually from TEM images with the software *ImageJ*. Figure 15 shows the interparticle distance distribution with a Gaussian fit, the mean value amounts to 3.0 ± 0.5 nm.

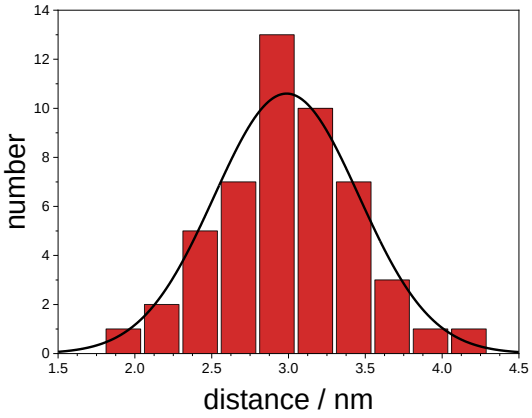


*Figure 15: Histogram and Gaussian distribution function of distances between CdSe NPLs in face-down orientation.*

Assuming that the capping ligands are attached evenly to all narrow facets, this value is lower than the length of two myristate molecules of 1.7 nm each[55], thus indicating an interpenetration of ligands of adjacent nanoplatelets. In total, square interface area of an individual CdSe NPL is $A_{NPL}$ = 200 nm$^2$ and the circular interface area of the Teflon well is $A_{well}$ = 177 mm$^2$. In a series of self-assembly experiments conducted according to the procedure for method II, either the volume $V$ or concentration $c_{NPL}$ was varied to increase the number of CdSe NPLs at the interface and thereby the theoretical surface coverage $x_{\%}$ of face-down monolayer films. Experimental parameters are listed in Table 1 and low magnification TEM images showing the size and structure of the respective monolayer films are depicted in Figure 16.

*Table 1: Overview of experimental parameters and theoretical surface coverage $x_{\%}$ for a series of self-assembly experiments by method II.*

| exp. | solvent | $c_{4ML}$ / mol·L$^{-1}$ | $V$ / µL | $x_{\%}$ / % | $T$ / °C |
|---|---|---|---|---|---|
| A | hexane | $2.95 \cdot 10^{-8}$ | 50 | 102 | 20 |
| B | hexane | $2.95 \cdot 10^{-8}$ | 60 | 120 | 20 |
| C | hexane | $3.52 \cdot 10^{-8}$ | 50 | 120 | 20 |

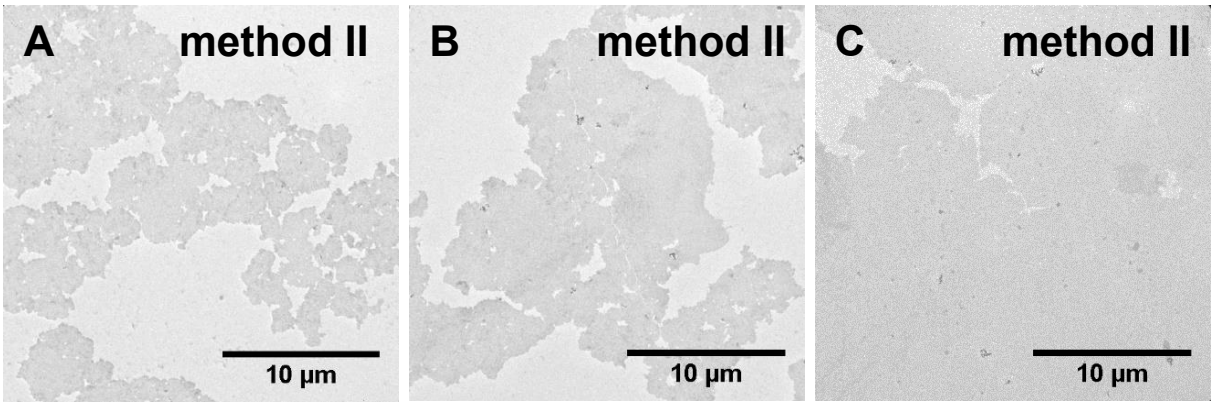


*Figure 16: TEM images of CdSe NPL face-down monolayer films obtained from self-assembly experiments by **method II**. Experimental conditions can be found in Table 1: Overview of experimental parameters and theoretical surface coverage $x_{\%}$ for a series of self-assembly experiments by method II.*

Although initial parameters should theoretically result in a complete coverage of the liquid interface with CdSe NPLs in face-down orientation, TEM images show a lower surface coverage of monolayer films (Figure 16A). This could be explained by the following considerations. On the one hand, the liquid interface hexane/air is not entirely flat but slightly curved, forming a concave meniscus due to the adhesion of the non-polar solvent to the Teflon well walls, effectively increasing the total surface area. On the other hand, while monitoring the self-assembly experiments under UV-Vis light, some CdSe NPLs were found to be deposited onto the inner walls of the Teflon well rather than to assemble at the acetonitrile/air interface. Thus the nanoplatelets are in fact spread over a larger surface area and as a result, the films on the TEM substrates exhibit a patchy structure. A higher theoretical surface coverage of 120% was achieved by increasing the volume $V$ from 50 µL to 60 µL (Figure 16B) or by increasing the concentration $c_{NPL}$ of the CdSe NPLs dispersed in hexane from $2.95 \cdot 10^{-8}$ mol/L to $3.52 \cdot 10^{-8}$ mol/L (Figure 16C). The films are coherent and significantly larger, usually covering entire 37 µm x 37 µm squares of the 400 mesh TEM grids while still maintaining an even thickness and consistent face-down orientation of CdSe NPLs. Therefore, optimized parameters of experiment C were used for subsequent self-assembly experiments. To ensure reproducibility of the results, experiments were repeated to prepare more face-down monolayer films, TEM images that attest to the improved quality and size of films can be found in Appendix 2.

## 3.5 Preparation of CdSe nanoplatelet monolayer films by method III

TEM images of films obtained by vertical deposition according to method III are depicted in Figure 17. In low magnification images, coherent films with sizes of up to 30 µm x 30 µm are visible (Figure 17A). Furthermore, folding of the monolayer films was observed. This is likely a result of an uneven deposition process as draining of the subphase was carried out manually and should be preventable for the automated transfer by Langmuir-Blodgett method. Furthermore, CdSe NPLs are deposited onto both sides of the substrate due to the dip-coating process of the CdSe NPLs film. This can be beneficial for some applications but complicates characterization of monolayer films by TEM. Places where both sides of the substrate are covered appear with higher contrast in TEM images but cannot be clearly distinguished from irregular or multilayered films deposited on only one side of the solid substrate. A major drawback of method III is a partial loss of control over CdSe NPL configuration for self-assembly experiments using CdSe NPLs dispersed in hexane. While most nanoplatelets are still kinetically trapped in the face-down configuration (Figure 17B), high magnification images reveal a significant increase of edge-up oriented nanoplatelets (Figure 17C).
Compared to method I and II, the Teflon well setup could not be covered with a glass dish to slow down the solvent evaporation rate in the beginning. Theoretically, omitting this step leads to a faster evaporation of solvent and should further favor the self-assembly of CdSe NPLs in the face-down orientation. Still, an open experimental setup is also more sensitive towards airflow above the interface, making it susceptible towards turbulences and fluctuations of the solvent evaporation rate in different places across the surface. This could explain an increase of CdSe NPL in an edge-up orientation.

In addition, it is important to consider the various draining and entraining forces associated with the vertical dip-coating process. When the subphase is drained from the Teflon well, the CdSe NPL film at the interface adheres to the substrate due to entraining effects, such as capillary forces. Draining forces caused by gravity, viscosity and surface tension draw the subphase solvent away from the substrate and back towards the bath. The balance between opposing forces depends on the withdrawal speed of the substrate and determines the thickness of the wet film.[56] In general, film thickness decreases with lower withdrawal speeds and increases again as soon as a critical value is undercut. At this point, the rate at which the wet film adheres to the substrate in the capillary regime is lower than the evaporation rate of the solvent and drying dynamics have to be considered, too.[56]

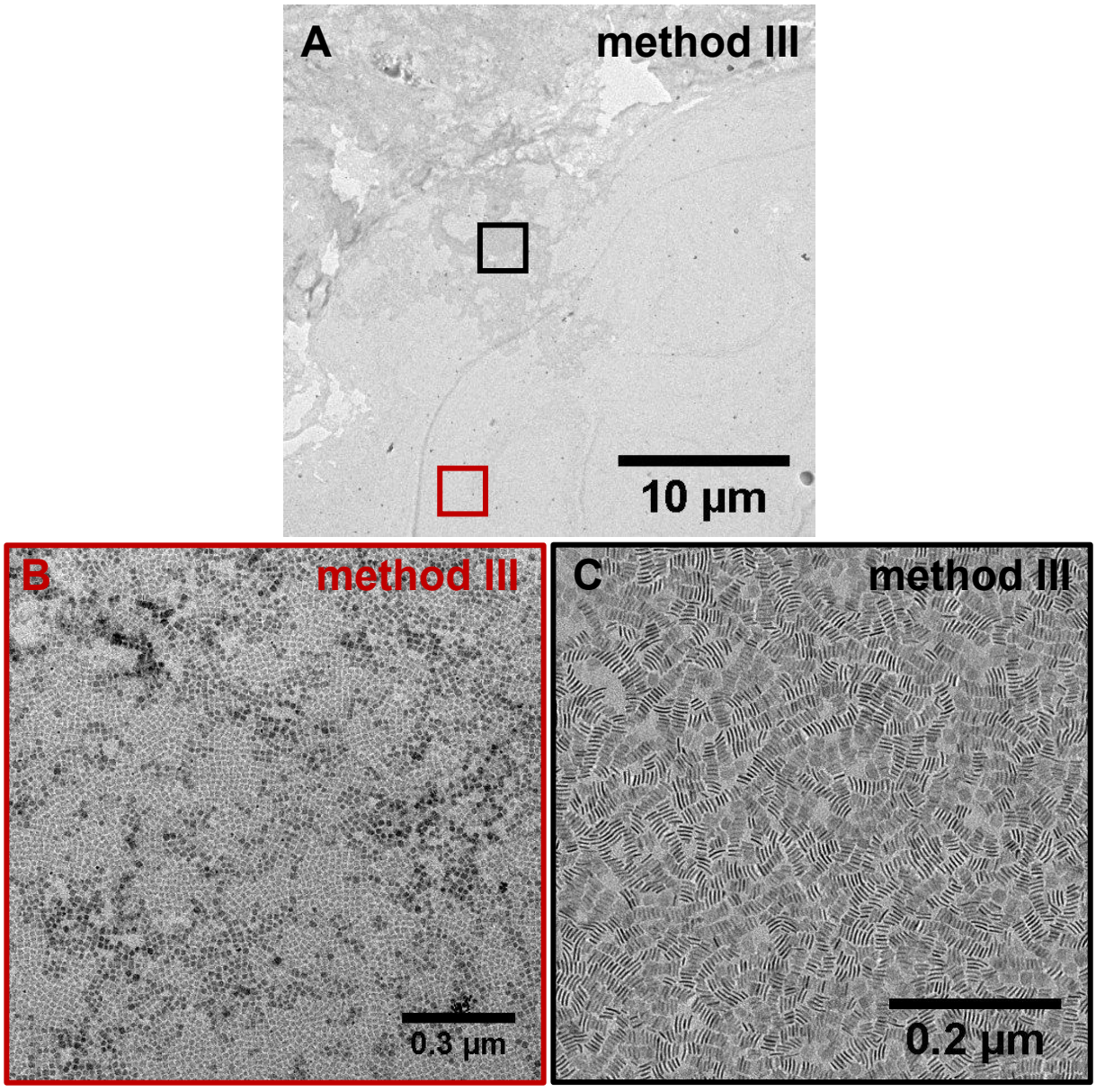


*Figure 17: TEM images of monolayer films prepared by **method III** from 4 ML CdSe NPLs dispersed in hexane (A-C). Images were recorded at different magnifications.*

Given that the subphase is drained manually for method III, withdrawal speeds are assumed to be above this limit. As a result, the wet film of acetonitrile solvent and CdSe NPLs on top should be relatively thick and, in combination with the vertical position, might allow for rearrangement of nanoplatelets during the drying process. Large monolayer films of purely edge-up oriented CdSe NPLs can be obtained by method III as shown in Figure 18. Upon closer inspection, nanoplatelet stacks of 100 nm on average are formed but they are packed less densely on the substrate surface (Figure 18B-C) in comparison to method I and II. Thus, while the evaporation of octane is still slow enough to yield a thermodynamically favored edge-up orientation of NPLs, this experimental procedure yields a lower degree of supramolecular order among nanoplatelet stacks.

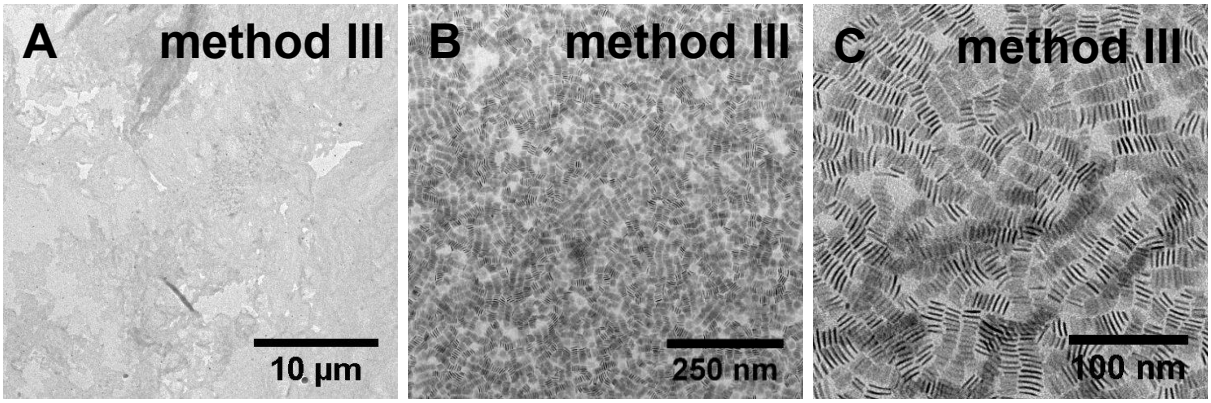


*Figure 18: TEM images of monolayer films prepared by **method III** from 4 ML CdSe NPLs dispersed in octane.*

In summary, self-assembly experiments by method III were successful in producing some coherent micro-sized monolayer films of CdSe NPLs. Yet TEM images reveal that method II is not as reliable for assembling nanoplatelets dispersed in hexane in an all face-down orientation. A possible explanation is connected to the speed of the vertical deposition process that determines the thickness of the wet film and could have an influence on the configuration of assembled CdSe NPLs, too. This hypothesis was reviewed by using a Langmuir-Blodgett setup which allows for better control of the deposition rate and enables a mostly jitter-free withdrawal of the solid substrate from the liquid phase.

## 3.6 Comparison of CdSe nanoplatelet film deposition methods I - III

In summary, monolayer films of CdSe NPLs were successfully prepared at the liquid interface and then transferred onto solid substrates. At a smaller scale, three different methods for film deposition were evaluated for self-assembly experiments in Teflon wells. The uniformity of nanoplatelet orientations as well as the size and surface coverage of the obtained films were evaluated and the best results were achieved with methods I and II in which films were transferred to the substrate surface in a horizontal manner. In method I, the substrate, a TEM grid, is placed on a level platform in the Teflon well and the final CdSe NPL film at the acetonitrile/air interface is slowly deposited by draining the acetonitrile subphase *via* a syringe.

In method II, a TEM grid is lowered into the subphase after self-assembly of CdSe NPLs and film formation and carefully lifted again to deposit the monolayer of nanoplatelets onto the substrate. Both methods yield homogeneous, at least 40 µm x 40 µm sized monolayer films with a high surface coverage and uniform configuration of CdSe NPLs. While good-quality films of edge-up oriented nanoplatelets were readily obtained from the beginning, the preparation of large and coherent face-down CdSe NPL monolayers proved more difficult as weaker attractive forces between narrow facets arise from the highly anisotropic shape of nanoplatelets. In addition, kinetic control over the self-assembly is ultimately more difficult to achieve than thermodynamic control, thereby impeding any efforts to obtain the kinetically favored face-down orientation. However, by adjusting the experimental procedure (*i.e.* increasing the concentration of nanoplatelets at the liquid interface, and thus contact between narrow CdSe facets), yielded significantly improved films. Vertical film deposition by method III resulted in similar-sized films of up to 35 µm x 30 µm but lead to a loss of control over the NPL configuration and no monolayers of purely face-down oriented nanoplatelets could be obtained in these experiments. Several explanations like irregular evaporation rates or a dependence of NPL orientation on deposition speed and wet film thickness were discussed but further experiments are necessary to review these assumptions and to gain a better understanding of the phenomenon but so far, vertical deposition methods have proven to be better-suited to monolayer film preparation from anisotropic CdSe NPLs.

## 3.7 Preparation of CdSe nanoplatelet monolayer films by Langmuir-Blodgett method

In this chapter, CdSe NPL self-assembly experiments were performed in a larger Teflon trough. In general, the Langmuir-Blodgett technique enables homogenous film deposition over large areas with precise control of the packing density and coating thickness.[44] Apart from the preparation of larger CdSe NPL monolayer films, two questions will be addressed in this section. In earlier self-assembly experiments, the face-down configuration of nanoplatelets was not maintained when monolayer films were deposited by method III, TEM images revealed a significant increase of edge-up oriented NPLs. Film deposition by Langmuir-Blodgett method should for more precise control of the deposition speed, and thereby the thickness of solvents films on the solid substrate. Withdrawing a solid substrate at a low and constant rate should lead to a thinner solvent film of remaining acetonitrile between the TEM grid surface and self-assembled CdSe NPL monolayer. This will reveal if the deposition speed impacts the configuration of nanoplatelets. Furthermore, the compression behavior of CdSe NPL monolayer films can be studied qualitatively to examine if the collective orientation of nanoplatelets can be modified *after* the self-assembly process by horizontal compression. To transfer the knowledge gained from self-assembly of CdSe NPLs in Teflon wells to Langmuir-Blodgett experiments, several parameters were scaled-up to fit the larger experimental setup. Figure 19 depicts a scheme of the experimental setup as well as a photograph indicating the dimensions of the Teflon trough. It holds a subphase volume of 120 mL and, depending on the deposition method, the surface area can adjusted in the range from 8.26 $cm^2$ - 12.27 $cm^2$. Using equation 3.3, the volume $V$ of colloidal CdSe NPLs that is required to cover a surface $A_{LBT}$ can be calculated.

$$V = \frac{A_{LBT} \cdot x_{\%} \cdot 100\%}{c \cdot A_{NPL} \cdot N_A} \quad (3.3)$$

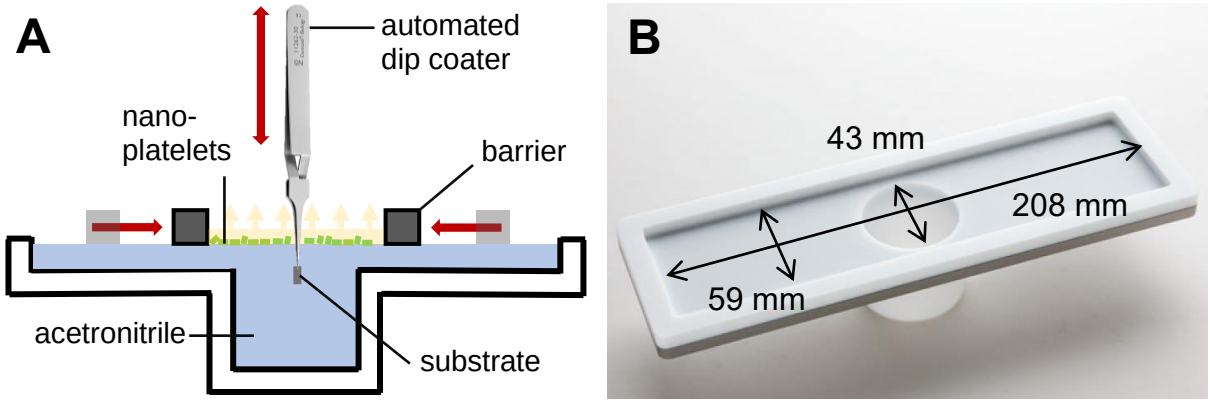


*Figure 19: Schematic representation of the experimental setup (A) and photograph of the Teflon trough used for the self-assembly of CdSe NPLs at the liquid interface by Langmuir-Blodgett method (B).*

By diluting aliquots from the same stock dispersion that was used for Teflon well experiments, the concentration of CdSe NPLs in hexane or octane was adjusted to $c = 3.5 \cdot 10^{-8}$ mol/L. The area of an individual nanoplatelet capped with myristate ligands was determined to be $A_{NPL}$ = 200 nm$^2$ in face-down configuration and $A_{NPL}$ = 60 nm$^2$ in edge-up configuration. In contrast to the Teflon well, calculations were performed assuming a theoretical surface coverage of 100% instead of 120%. This is reasonable when considering that films can be further condensed by barrier compression if necessary. A summary of experimental parameters of all Langmuir-Blodgett experiments is listed in Table 2.

*Table 2: Overview on experimental parameters for self-assembly experiments by Langmuir-Blodgett method.*

| exp. | $A_{LBT}$ / mm$^2$ | orientation | $V$ / µL | $T$ / °C | $v_d$ / mm · min$^{-1}$ | $c_{rate}$ / mm · min$^{-1}$ |
|---|---|---|---|---|---|---|
| LB-1a | 1601 | face-down | 371 | 20 | 1 | - |
| LB-1b | 1601 | edge-up | 1238 | 20 | 10 | - |
| LB-2a | 826 | face-down | 192 | 20 | - | - |
| LB-2b | 826 | edge-up | 667 | 20 | - | - |
| LB-3a | 826 - 3304 | mixed | 192 | 20 | - | 1 mm/min |
| LB-3b | 826 - 3304 | mixed | 639 | 20 | - | 1mm/min |

### 3.7.1 Controlled deposition of CdSe nanoplatelet monolayer films by method III

In Teflon wells, vertical film deposition according to the procedure of method III resulted in mixed configurations of NPLs in monolayer films prepared from dispersions in hexane. As the experimental setup could not be covered in method III, the self-assembly process of CdSe NPLs at the liquid interface was more susceptible towards airflow and fluctuating evaporation rates which could explain the observation of edge-up oriented nanoplatelets. Also, the film was transferred onto the solid substrate by manually draining the acetonitrile subphase *via* a syringe and without control over the deposition speed. This is important to note as the deposition speed directly impacts the thickness of the acetonitrile solvent layer between assembled nanoplatelets and the solid substrate.[56] Thicker solvent layers can result from fast deposition and require more time to evaporate, thus possibly enabling a partial rearrangement of CdSe NPLs. Vertical film deposition by Langmuir-Blodgett method should help to review these assumptions since the Teflon trough setup can be covered and the automated dip coater allows for precise control of deposition speed.

First, two self-assembly experiments of CdSe NPLs with film deposition by Langmuir-Blodgett method were carried out at a constant trough area of $A_{LBT}$ = 16.01 cm$^2$ which had been adjusted with compression barriers beforehand. After adding the acetonitrile subphase to the trough and immersing the substrate below the surface area, CdSe NPLs dispersed in hexane were slowly spread on top and the trough setup was immediately covered to reduce air flow above the liquid interface and prevent fluctuations in the evaporation rate of hexane. A minor decrease in surface tension of $\Delta\gamma$ = 2.1 mN/m was observed upon application of the CdSe NPL dispersion to the interface. This is a result of the preferred interaction of non-polar capping ligands with both air and acetonitrile. After complete evaporation of the solvent, film deposition was started in constant pressure mode and the substrate was vertically lifted from the trough at a constant speed of either $v_d$ = 1 mm/min or $v_d$ = 10 mm/min. Figure 20 shows TEM images of the resulting monolayer films. At a slow deposition speed of 1 mm/min, coherent films reach up to 300 µm$^2$ in size. Still, the shape of the film edges in high magnification TEM images (Figure 20A) suggests that these are fragments of larger films which fractured, *e.g.* during deposition. When transferring the film onto the substrate at a significantly higher speed of 10 mm/min, the monolayer breaks up in even smaller fragments (Figure 20C). Although the film was deposited in constant pressure mode, meaning that any changes in the surface pressure during deposition are compensated by the barriers, strain caused by the vertical lifting process could not be lowered enough to prevent tearing of the monolayer. This clearly demonstrates that deposition at lower speeds is necessary for obtaining coherent monolayer films. Yet, vertical deposition by Langmuir-Blodgett method results in a loss of control over the NPL configuration, as is evident from TEM images at higher resolutions (Figure 20B, D). For both experiments performed with a film deposition speed of $v_d$ = 1 mm/min or $v_d$ = 10 mm/min, a mixture of face-down and edge-up oriented CdSe NPLs was observed. Notably, both configurations were found across the entire substrate surface instead of in separate domains. Compared to self-assembly experiments by method II in Teflon wells, the Langmuir-Blodgett trough was covered during part of the solvent evaporation process, thereby minimizing airflow above the liquid interface.

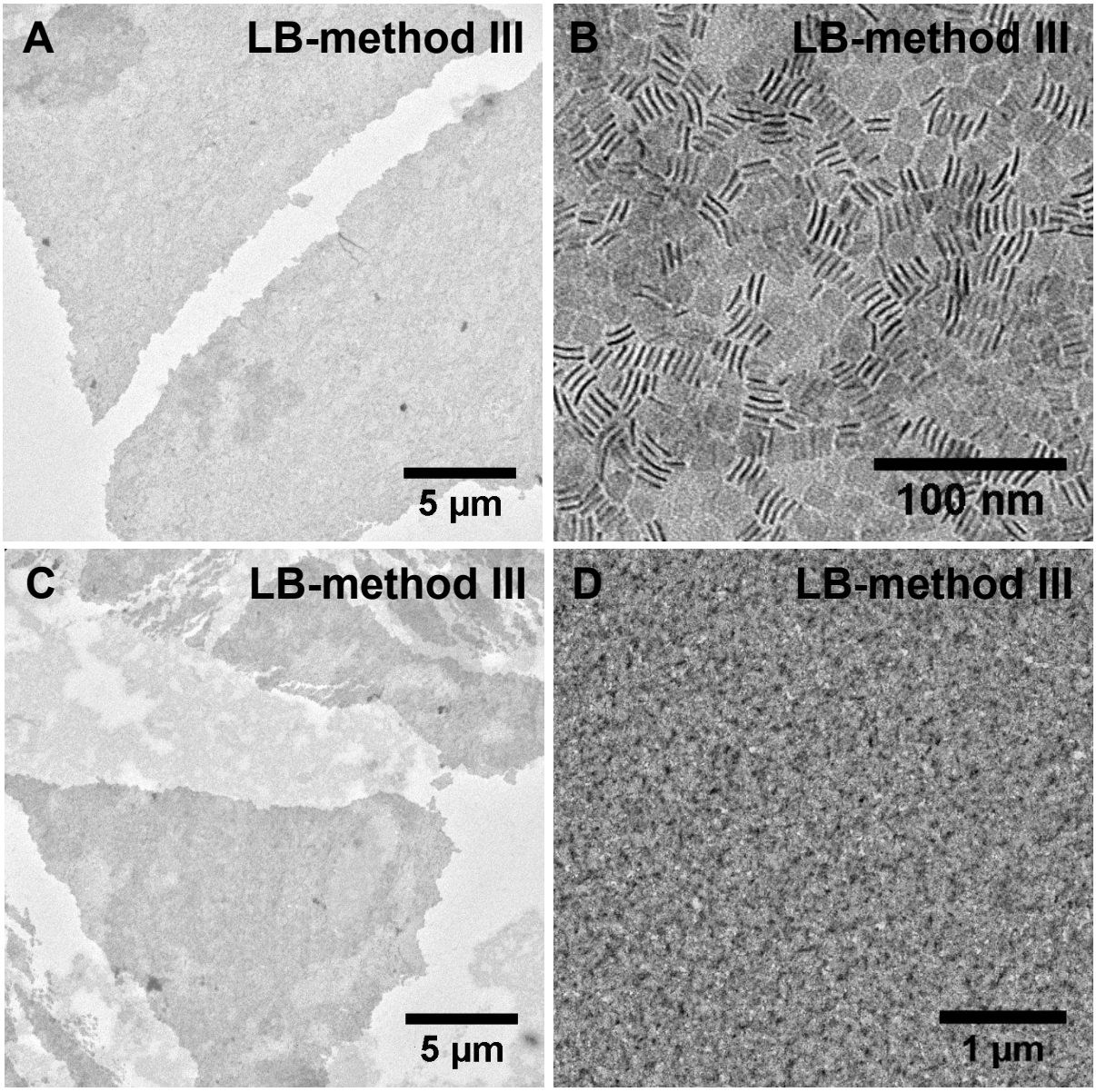


*Figure 20: TEM images of CdSe NPL monolayer films deposited by Langmuir-Blodgett method in LB-1a (A-B) and LB-1b (C-D). The deposition speed was varied between 1 mm/min (A-B) and 10 mm/min (C-D)*

On this account, turbulences and fluctuations of evaporation rate are unlikely to cause an inconsistent configuration of CdSe NPLs.According to literature, the withdrawal speed of film deposition is directly connected to the solvent layer thickness which was also presumed to influence the collective orientation of nanoplatelets. However, the films which were deposited at $v_d$ = 1 mm/min (LB-1a) and $v_d$ = 10 mm/min (LB-1b) do not differ in terms of NPL configuration, both showing a mixture of face-down and edge-up oriented nanoplatelets.
Additional Langmuir-Blodgett experiments at intermediate deposition speeds are necessary to verify if it correlates with the orientation of CdSe NPLs in monolayer films. Overall, the results from self-assembly experiments in Teflon wells by method II as well as LB-1a and LB-1b suggest that horizontal deposition methods are better suited to transfer of CdSe NPL monolayer to solid substrates.

In this regard, a similar method called Langmuir-Schäfer[57] might be better suited to the deposition of coherent monolayer films with uniform CdSe NPL orientation and can be implemented with the Teflon trough setup.

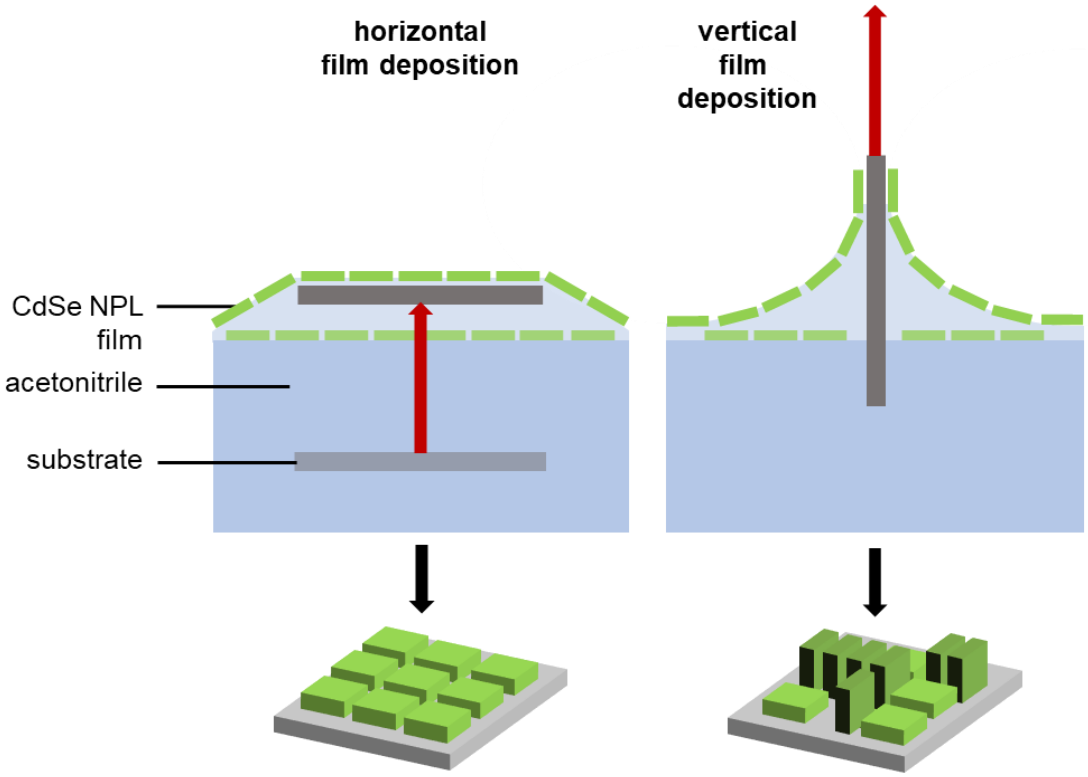


*Figure 21: Impact of film deposition method on final configuration of CdSe NPLs on substrate. Horizontal deposition maintains face-down configuration of nanoplatelets, vertical deposition yields mixtures of face-down and edge-up oriented CdSe NPLs on the substrate.*

## 3.7.2 Self-assembly and horizontal deposition of films in a Langmuir-Blodgett trough

The Langmuir-Blodgett trough setup was combined with a horizontal film deposition according to method II in order to verify if the self-assembly experiments of CdSe NPLs at the liquid interface are practicable on a larger scale and if the collective orientation of CdSe NPLs can be maintained with the Teflon trough setup. Therefore, a face-down monolayer film was prepared from colloidal CdSe NPLs in hexane (LB-2a) and another monolayer film with edge-up oriented nanoplatelets was prepared from colloidal CdSe NPLs in octane (LB-2b). Acetonitrile was added to the trough as a subphase and the trough area was adjusted by barrier compression to $A_{LBT}$ = 8.26 cm$^2$ which is more than four times as large as the interface area in Teflon wells of $A_{well}$ = 1.77 cm$^2$. Then, CdSe NPLs dispersed in the respective alkane solvent were carefully spread on the interface and the trough setup was covered to ensure a controlled evaporation of the dispersion. After self-assembly of nanoplatelets and film formation, the cover was removed and a TEM grid, held by a pair of tweezers, was manually immersed in the trough and horizontally lifted upward to deposit the assembled CdSe NPLs onto the substrate surface. Representative TEM images are included Figure 22.

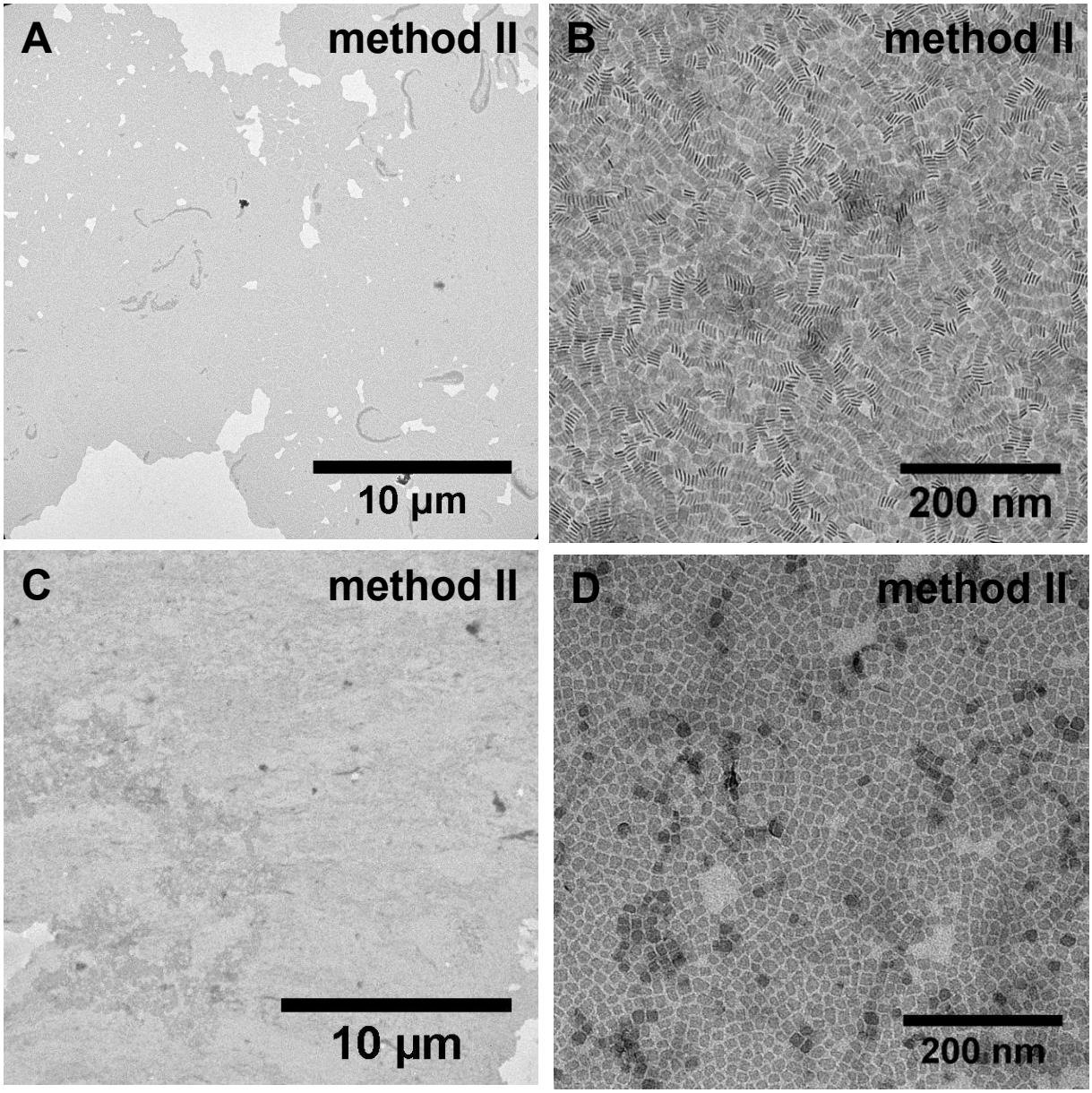


*Figure 22: TEM images of monolayer films prepared by Langmuir-Blodgett method in experiments LB-2a and LB-2b. CdSe NPLs are oriented in edge-up in experiment LB-2b (A-B) or face-down in LB-2a (C-D).*

In both cases, large coherent monolayer films of at least 500 $\mu m^2$ were obtained and a collective orientation of CdSe NPLs was maintained over the entire substrate surface. Hence, these experiments demonstrate that this method of self-assembling nanoplatelets at the liquid interface and controlling their configuration by kinetic effects of solvent evaporation can be applied to a larger scale, thereby enabling the coating of various larger substrates in future work.

### 3.7.3 Compression behavior of CdSe nanoplatelet monolayer films

After having gained control over the collective orientation of CdSe NPLs, the two barriers of the Langmuir-Blodgett setup were horizontally compressed after the self-assembly of CdSe NPLs at the liquid interface to analyze the compression behavior of monolayer films (LB-3a). Nanoplatelets dispersed in hexane were applied to a trough area of $A_{LBT}$ = 33.04 cm$^2$, giving a theoretical surface coverage of 25% of face-down monolayer film. Then, horizontal barrier compression was started at a rate of $c_{rate}$ = 1 mm/min, continuing until the trough area was reduced to $A_{well}$ = 8.26 mm$^2$ at which point the theoretical surface coverage by face-oriented NPLs should be 100%. A low compression rate was chosen in order to enable particle rearrangements, if necessary, thus giving nanoplatelets enough time to re-arrange and adjust to the constantly decreasing area of the Teflon trough. TEM grids were manually coated with the film at different stages during the compression process by immersing the substrate into the acetonitrile phase below the assembled monolayer film and then lifting it upwards again. Also, a compression isotherm was recorded *via* the wire probe at the liquid interface. Representative images of monolayer films with varying surface coverage as well as the compression isotherm are depicted in Figure 23.

At low surface concentrations, CdSe nanoplatelets are oriented face-down and form individual, worm-like structures (Figure 23Figure 22B) that are likely spread across the entire trough area. The observation of assembled structures rather than individual particles suggests that any attractive forces between CdSe NPLs, even between their narrow facets, are strong enough to form small, elongated islands of nanoplatelets in face-down orientation. Upon further compression, the worm-like structures become interconnected thereby forming a network of face-down oriented CdSe NPLs (Figure 23C), some NPLs were also observed to lie on top of each other. At high surface concentrations, the CdSe NPL film is clearly more condensed but also more irregular in thickness as can be seen from low magnification TEM images. Whereas parts of the substrate were not covered with nanoplatelets, double-layered and edge-up oriented NPLs were also found in some regions (Figure 23B). Due to the network-like structure of the film, CdSe NPLs at linking points should experience stronger repulsive forces because they are entirely surrounded by other nanoplatelets, whereas NPLs in bridging parts of the network can be moved to free areas of the interface. Figure 24 shows a low magnification TEM image (Figure 24B) of the final monolayer film obtained in this experiment (LB-3a), films cover entire squares of the substrate which are 37 µm x 37 µm in size. Furthermore, domains with CdSe NPLs in edge-up configuration (Figure 24C) can be clearly distinguished from face-down oriented nanoplatelets (Figure 24A). The size of these domains varies within the nm and low µm range. The compression isotherm (Figure 23A) can be divided into the following two sections: Up to 75% theoretical face-down surface coverage (at a trough area of $A_{LBT}$ = 11.00 cm$^2$), the surface pressure at the interface increases linearly with a decrease in trough area. Above this value, the slope of the isotherm is steeper, indicating stronger repulsion between CdSe NPLs. In order to minimize repulsive forces between nanoplatelets in face-down configuration, NPL monolayers can either be pushed over another monolayer, resulting in double-layered structures, or rearrange into edge-up orientation, which requires a smaller surface area per individual nanoplatelet.

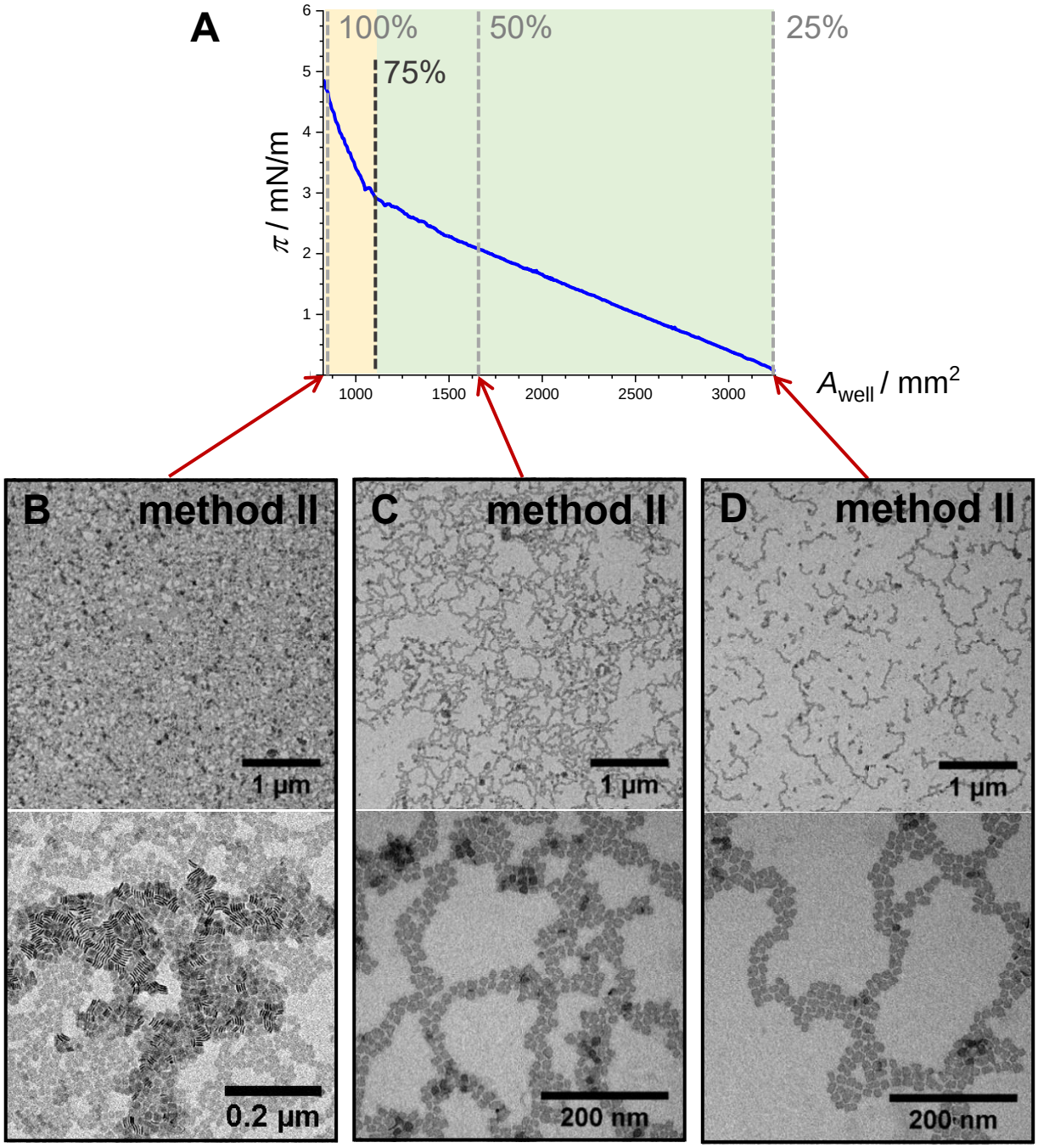


*Figure 23: Compression isotherm of LB-3a (A) and TEM images of CdSe NPL monolayer film (B-D) during barrier compression at a rate of 1 mm/min. Substrates were coated with films at a theoretical surface coverage of 25% (B), 50% (C) and 100% (D) by face-down oriented NPLs.*

This could also depend on the compression rate. If horizontal compression occurs faster than the re-arrangement of CdSe NPLs from face-down to edge-up configuration, multi-layered structures should be obtained. However, this experiment clearly demonstrates that a change of the collective orientation of CdSe nanoplatelets can be caused by horizontal compression at low compression rates. Edge-up oriented NPLs were observed to form small, defined regions rather than occurring individually. This was assumed to result from the heterogeneous distribution of nanoplatelets on the liquid interface.

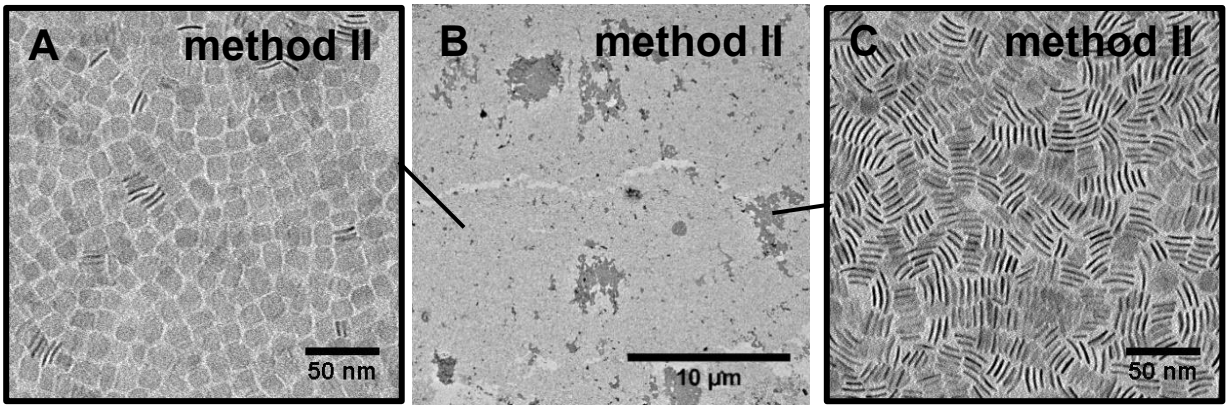


*Figure 24: TEM images of a CdSe NPL monolayer film (A-C) in experiment LB-3a at 100% theoretical surface coverage for face-down oriented NPLs Images show regions of edge-up oriented nanoplatelets within a film mostly made of CdSe NPLs in face-down orientation. Barrier compression rate was 1mm/min.*

This also implies that an extensive change in the configuration of CdSe NPLs in monolayer films could be evoked by slow horizontal compression of a film with high surface coverage and a homogeneous distribution of nanoplatelets. Then, all CdSe NPLs are entirely surrounded by other NPLs and should experience equally strong repulsive forces upon compression of the monolayer film. Therefore, a larger volume of colloidal CdSe NPLs was applied to an area of $A_{LBT}$ = 33.04 mm$^2$ so that the initially formed film already had a surface coverage close to 100%, resulting in a more even distribution of nanoplatelets at the interface (LB-3b). In the next step, barrier compression was started at $c_{rte}$ = 1 mm/min, monolayer films of self-assembled CdSe NPLs were compressed beyond a theoretical surface coverage of 100% to reveal if the share of edge-up oriented NPLs could be further increased. Also, a compression isotherm was recorded in this experiment. As soon as the trough area was reduced to the minimum value of $A_{LBT}$ = 8.26 cm$^2$, a TEM grid was coated with the compressed film of CdSe NPLs by immersing the substrate into the acetonitrile phase below the assembled monolayer film and then lifting it upwards again. TEM images of the CdSe NPL monolayer film are depicted in Figure 25. CdSe NPLs assembled both in face-down and edge-up configuration without formation of clearly defined domains (Figure 25A). Overall, an increase of edge-up oriented nanoplatelets was observed. The slope of the compression isotherm steadily increases as the trough area is reduced, but an onset of the change in NPL orientation cannot be specified from the data. It can expected that this process advances steadily rather than taking place at a specific surface pressure or surface coverage.

Lastly, the behavior of a compressed CdSe NPL film upon slow barrier relaxation was studied in the same experiment to reveal how a decrease in surface pressure affects the orientation of compressed nanoplatelets. Starting at a trough area of $A_{LBT}$ = 8.26 cm$^2$, barriers relaxation was started at a rate of 1 mm/min and continued until the trough area had increased to the initial value of $A_{LBT}$ = 33.04 cm$^2$. During the first part of barrier relaxation, a significantly greater change in surface pressure was measured than during the last part of barrier compression. At a trough area of $A_{well}$ = 10.00 cm$^2$, $\pi$ falls below zero and continues to decrease further, albeit to a lesser extent. Ultimately, a difference of $\Delta\pi$ = -3 mN/m was observed in comparison to the beginning of the experiment.

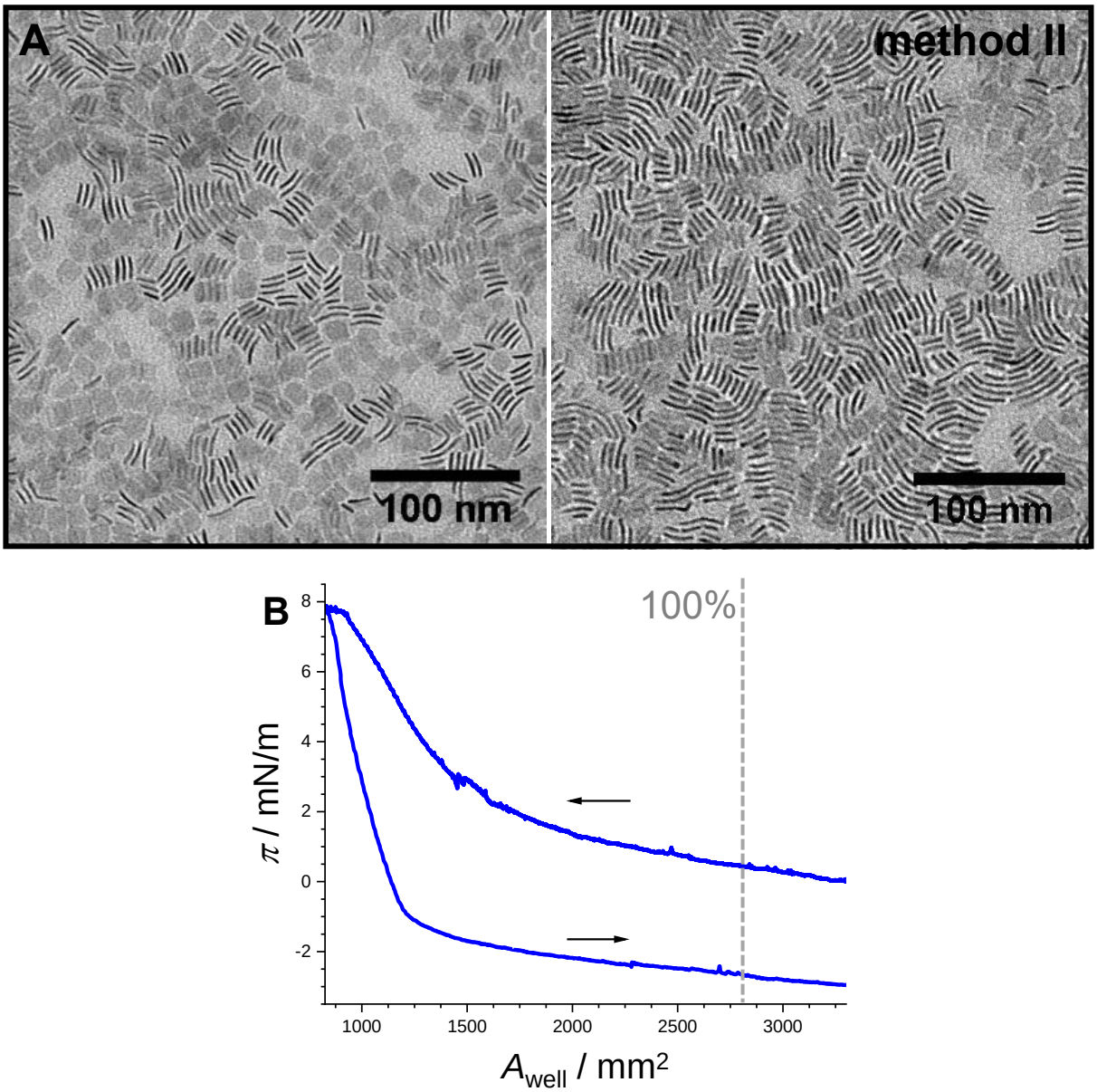


*Figure 25: High magnification TEM images of a CdSe NPL monolayer film from after horizontal compression at a rate of 1 mm/min (A). Compression isotherm of experiment LB-3b (B), showing hysteresis behavior of the NPLs.*

Thus, the monolayer film of CdSe NPLs clearly demonstrates hysteresis behavior. Upon horizontal compression, a large number of nanoplatelets adopted the stable edge-up orientation, yielding short stacks composed of 2-10 NPLs that are held together by attractive forces between their wide facets. Another change back to face-down orientation would be energetically unfavorable and is therefore not expected to occur. The difference in surface pressure at $A_{well}$ = 33.04 cm$^2$ stems from the lower surface area required for an individual nanoplatelet in edge-up orientation, leaving part of the liquid interface uncovered that was initially covered with face-down oriented NPLs.

All in all, this experiment demonstrated that horizontal compression of CdSe NPLs monolayer films causes a non-reversible change in nanoplatelet orientation from face-down to edge-up.

In self-assembly experiments with low surface concentrations of NPLs, barrier compression yields films with a network-like structure that can be further condensed and eventually show segregated domains of edge-up oriented CdSe NPLs. In contrast, films with homogeneous distribution and high surface coverage of NPLs results in area-wide configurational changes of the CdSe NPLs.

### 3.7.4 Summary of Langmuir-Blodgett self-assembly experiments of CdSe nanoplatelets

Overall, CdSe NPLs were successfully assembled at the liquid interface of a Langmuir-Blodgett trough and large films with uniform orientation of nanoplatelets were deposited onto TEM grids by horizontally lifting the substrate from the subphase below the monolayer film. The experimental procedure was adjusted to a Langmuir-Blodgett trough setup, thereby enabling large-scale preparation and transfer of CdSe NPL films onto a variety of different solid substrates. Furthermore, Langmuir-Blodgett experiments including a compression by barriers indicate that a non-reversible change of the nanoplatelet orientation from face-down to edge-up can be induced by horizontal compression of monolayer films at the liquid interface. However, a certain fraction of CdSe NPLs was still oriented face-down in the monolayer films. Additional experiments could reveal if a purely edge-up oriented NPLs can be obtained in this manner. For example, this might be achieved by using larger volumes of colloidal CdSe NPLs (to compensate possible material losses at the Teflon boundaries) or by reducing the available trough area for nanoplatelets even further.

## 3.8 Preparation of double layer films by self-assembly of CdSe nanoplatelets

Developing a succesful and reliable procedure for the preparation of homogeneous CdSe NPL monolayer films paves the way towards double-layered or even multi-layered structures. Research has shown that highly ordered assemblies of semiconductor nanoplatelets exhibit collective properties that are beneficial to various optoelectronic applications. Since face-to-face stacking is a commonly observed feature in these anisotropic materials[3], many groups have studied optical properties of CdSe NPL stacks, ranging from phonon coupling at low temperatures[58] to efficient homo-FRET between identical nanoplatelets[59] or FRET between nanoplatelets of different thicknesses.[7,24]
Double-layer films of CdSe NPLs in which both layers are composed of face-down oriented nanoplatelets are, effectively, numerous stacked NPL pairs distributed over a certain area. Such a structure allows for studying energy transfer processes between two individual nanoplatelets rather than in a long stack composed of multiple NPLs. In this project, double-layered films with controlled orientation of CdSe NPLs were prepared in in Teflon wells by succesively depositing two monolayers onto a solid substrate by method I or II. In total, self-assembly experiments of colloidal CdSe NPLs dispersed in hexane or octane were conducted in every possible order to yield four types of double layer films, face-down/face-down (FD-FD), face-down/edge-up (FD-EU), edge-up/face-down (EU-FD) and edge-up/edge-up (EU-EU) films are illustrated in Figure 26.

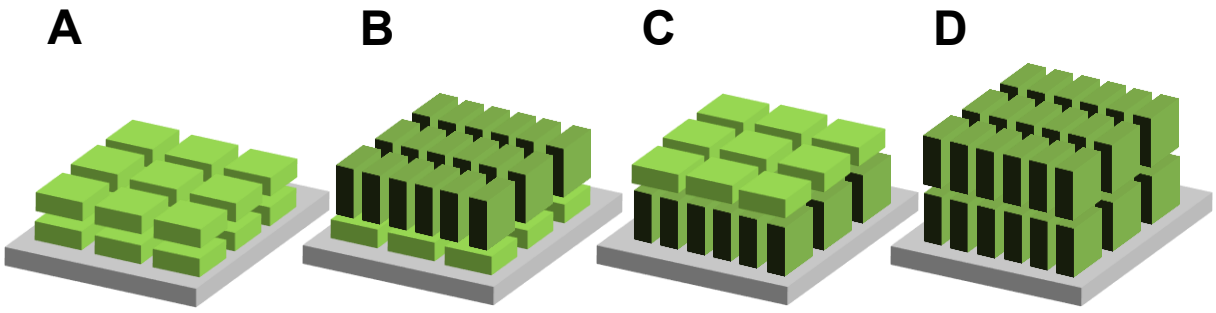


*Figure 26: Schematic representation FD-FD (A), FD-EU (B), EU-FD (C) and EU-EU (D) double layer films of CdSe NPLs.*

For the preparation of double-layer films, a first self-assembly experiment of CdSe NPLs was carried out according to method II. After the complete evaporation of alkane solvent, a TEM grid was carefully lowered into the acetonitrile layer using a pair of tweezers and removed again in an upward motion, thereby transferring the CdSe NPL film from the liquid interface onto the solid substrate. Monolayer films were then analyzed by transmission electron microscopy before proceeding with the deposition of the second nanoplatelet layer on top by method I. In this procedure, the TEM grid coated with a monolayer film was immersed in the acetonitrile subphase and placed on a level platform in the Teflon well.
Then, colloidal CdSe NPLs were added, the alkane solvent was allowed to evaporate completely and the formed film was transferred onto the susbtrate by slowly draining the the subphase. Method I was chosen for this step because it caused fewer disruptions to the film on the TEM. Method II sometimes resulted in folded edges of CdSe NPL films, likely due to unintentional variations in the angle at which the substrate was lowered into the Teflon well. TEM images of the final double layer films with a FD-EU, EU-FD and EU-EU structure are shown in Figure 27.
At high magnifications, the respective orientations of CdSe NPLs in both the upper and lower monolayer are visible for EU-EU (Figure 27A), thus confirming that a preparation of double layer films by consecutive deposition of CdSe NPL monolayers is generally possible. Combinations of EU-FD (Figure 27B) and FD- EU nanoplatelets (Figure 27C) are difficult to distinguish from these images due to the limited resolution of the TEM in z-direction. Likewise, the structure of double-layered films cannot be readily identified in low magnifications images as any differences in contrast are too low between dissimilar structures. In this case, additional characterization of the sample surface by scanning probe microscopy methods, such as atomic force microscopy, could be helpful for mapping the topology of double layer films. Height profiles of nanoplatelets in face-down orientation should show lower steps at the film edges and between individual layers when compared to those of nanoplatelets in edge-up orientation. In addition, this could also enable a quantification of the surface coverage of double layer films. However, any attempts to prepare FD-FD films from CdSe NPLs dispersed in hexane yield double-layer films in which numerous nanoplatelets in the upper layer adopted the edge-up configuration (Figure 27D).

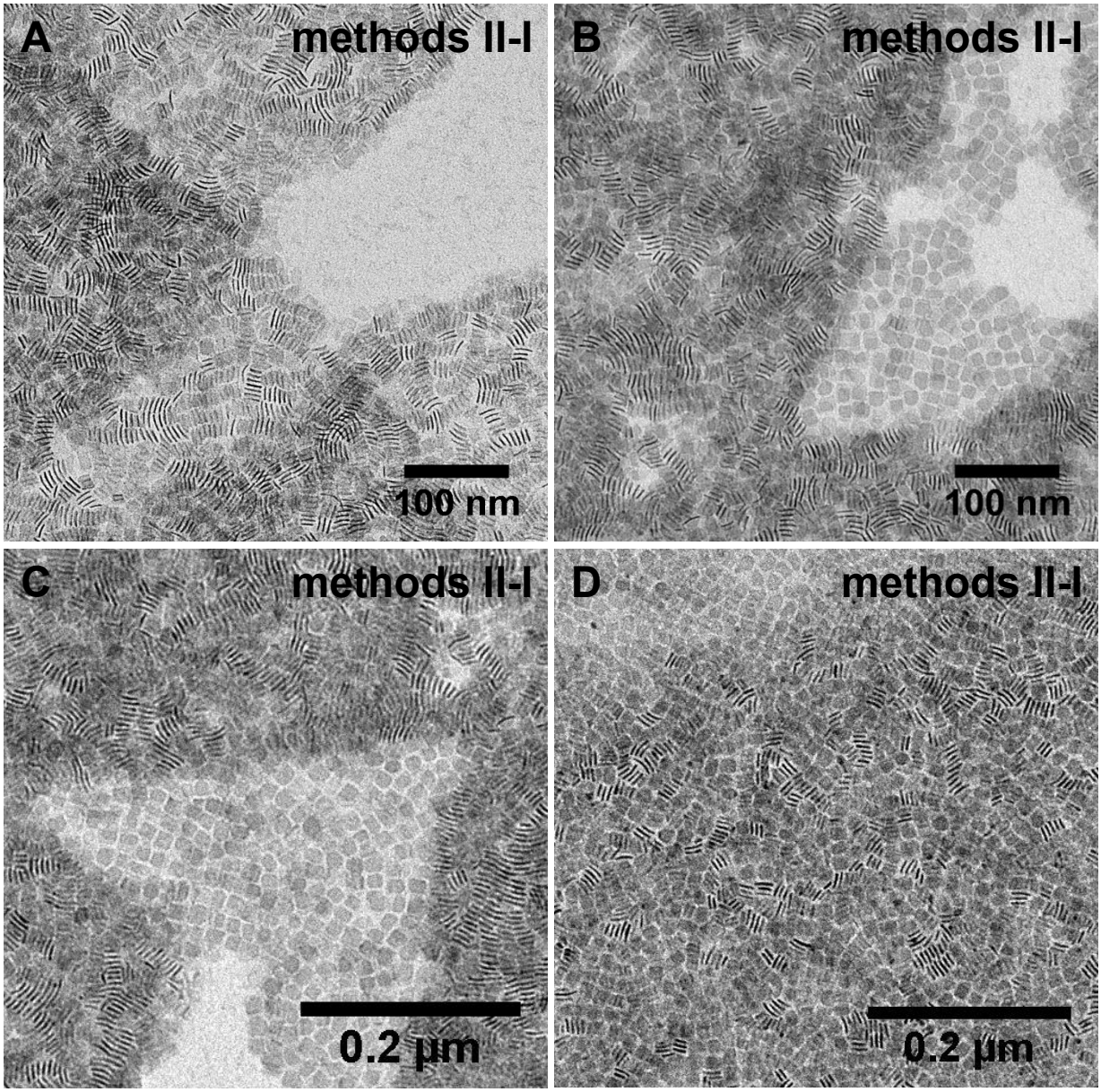


*Figure 27: TEM images of double layer films of CdSe NPLs. Nanoplatelets are oriented EU/EU (A), EU-FD (B) and FD-EU (C). Numerous CdSe nanoplatelets in the top layer of FD-FD films are oriented edge-up.*

At this point, there are two possible explanations, both are illustrated in Figure 28. In the setup of method I, a TEM grid coated with a face-down monolayer of CdSe NPLs is placed on the platform in the center of the Teflon well. First, mirstate ligands detach from the surface of the CdSe NPLs on the solid substrate during self-assembly experiments in acetonitrile and migrate to the acetonitrile/hexane interface, thereby affecting the self-assembly of nanoplatelets. In a similar scenario, GAO *et al.*[4] demonstrated that the intentional addition of small amounts oleic acid to a diethylene glycole subphase promote the edge-up assembly of CdSe NPLs. This would imply that NPLs assemble in the edge-up orientation before deposition onto the substrate. Second, initially face-down oriented nanoplatelets in the top layer rearrange when approaching the nanoplatelet layer on the TEM grid during the deposition process. In this context, it should be noted that the deposition of myristate-capped CdSe NPLs onto another layer of nanoplatelets represents a different situation than the deposition onto a solid substrate such as carbon-coated copper TEM grids

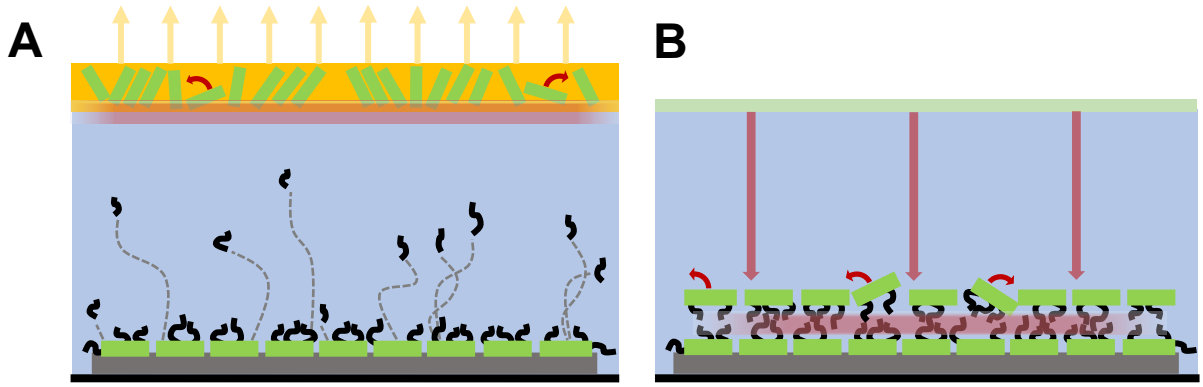


*Figure 28: Schematic representation of two possible mechanisms leading to a partial to edge-up orientation of CdSe NPLs in double layer films. Nanoplatelets either assemble edge-up at the interface due to detachment of myristate ligands and altered interaction potentials (A) or rearrange during deposition due to repulsive ligand interactions*

In the first case, repulsive forces stemming from the interpenetration of ligands shells around nanoplatelets have to be considered. Dense ligand brushes cause strong repulsions between NPLs and decelerate the stacking process, that is, nanoplatelets require a longer time to adopt the face-to-face configuration.[3] In this project, the coverage of CdSe NPLs with myristate ligands was calculated from TGA data and amounts to 4 per $nm^2$. The ligands are bound to cadmium atoms of the terminating CdSe zincblende lattice. Due to the highly anisotropic shape of nanoplatelets, a great share of myristate molecules should be located on wide (100) facets. Considering a lower steric hindrance of ligands on narrow (001) and (010) facets as well as the smaller area of these facets, the preparation of EU/EU, EU/FD and FD/EU double layers of CdSe NPLs should be less hindered by ligand interactions. This is exactly what was observed in self-assembly experiments.

To verify these hypotheses and to determine at which point nanoplatelets adopt the edge-up configuration, during self-assembly or during film transfer, the following control experiment was conducted. A TEM grid coated with a face-down monolayer film of NPLs was placed on the Teflon well platform in acetonitrile, then CdSe NPLs dispersed in hexane were applied to the liquid interface. After self-assembly of nanoplatelets and evaporation of hexane solvent, the resulting film was deposited onto a second TEM grid. Images of the monolayer film on the second substrate and a scheme of the control experiment are included in Figure 29. Therefore, the detachment of myristate ligands and change of the interaction potential between subphase and CdSe NPLs was not the cause of the edge-up orientation of many nanoplatelets in the double layer film. This is further supported by previous studies, short-chain alcohols induce a release of carboxylate ligands from the surface of CdSe nanoparticles but acetonitrile does not.[60] Both, short-chain alcohols and acetronitrile are commonly used as antisolvents in the purification process of crude semiconductor nanoparticles and HASSINEN *et al.* intepreted the different behavior as a result of their protic or aprotic character. Detachment of carboxylate ligands is assumed to proceed *via* deprotonation of solvent followed by proton transfer to the capping ligand, hence only protic alcohols can provide the protons required to detach carboxylate ligands. As CdSe nanoplatelets were indeed observed to assemble face-down at the liquid interface, the change in orientation has to take place during the deposition of the film onto the monolayer on the substrate. If repulsive interactions between surface ligands of CdSe NPLs in the two layers cause a partial rearrangement of nanoplatelets, then removal of myristate ligands on CdSe NPLs on the solid substrate or substitution with short-chain ligands should facilitate the deposition process and maintain the collective face-down orientation. In case of colloidal CdSe QDs, stripping of X-type ligands is achieved by addition of protic solvents like methanol or ethanol.[60,61]

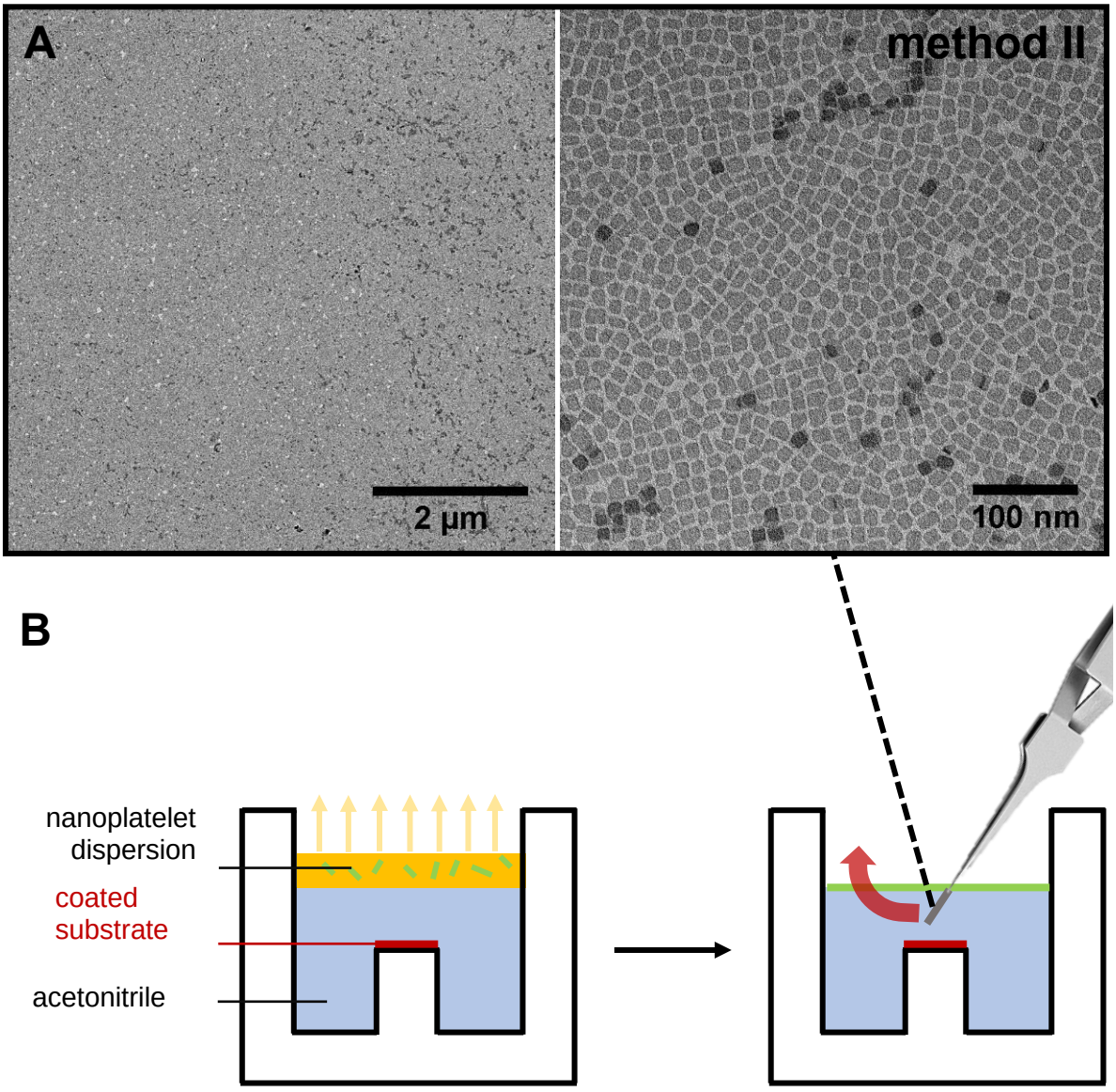


*Figure 29: TEM images of monolayer film on second TEM grid, CdSe NPLs are clearly assembled in face-down orientation at the interface (A). Scheme of control experiment with coated substrate in Teflon well (B).*

In order to adopt this approach, TEM grids coated with one monolayer of face-down oriented NPLs were individually placed in glass vials with methanol or ethanol for several hours, then thoroughly rinsed with the respective solvent and dried before proceeding with the application of a second CdSe NPL monolayer. TEM images of a treated CdSe NPL monolayer film (Figure 30A) and resulting double layer film (Figure 30B) are shown in Figure 30. This procedure proved succesful in preparing double layer films of CdSe NPLs with good surface coverage and uniform face-down orientation of nanoplatelets. The size of films was estimated from low magnification TEM images (Figure 30C-D) and amounts to 50-75 µm$^2$. For future work, it would also be insightful to determine the fraction of the substrate surface covered with a monolayer and double layer CdSe NPL film, for example by AFM measurements and analysis of recorded topological images. These experiments were repeated to ensure reproducibility of the procedure for double layer film preparation. Unfortunately, the top layer sometimes included CdSe NPLs in edge-up orientation. This could be related to the washing step with methanol and ethanol which could be optimized in future work.

Colloidal CdSe QDs can be analyzed by $^{1}$H-NMR spectroscopy and UV-Vis spectroscopy[62] to verify and quantify the stripping of carboxylate ligands but both characterization methods cannot readily be applied to QDs or NPLs on solid substrates.

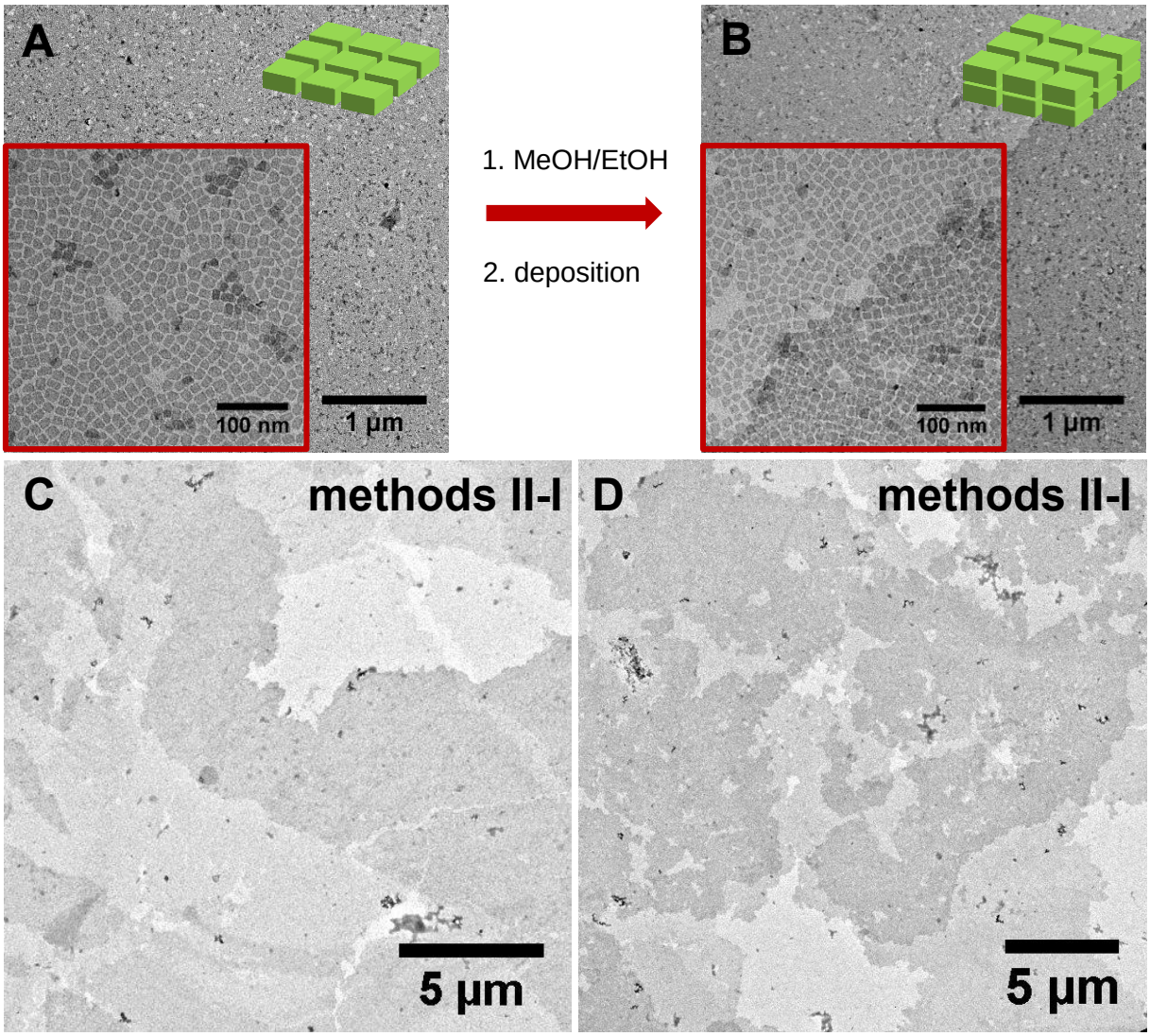


*Figure 30: CdSe NPL monolayer film treated with MeOH (A) and resulting double layer film with CdSe NPLs oriented face-down in both layers (B). Low magnification TEM images of double layer films (C-D).*

It was also theorized that the washing step merely removed impurities from the coated TEM grids which affected the deposition process. In general, self-assembly experiments of CdSe NPLs at the liquid interface are highly susceptible to very low amounts of impurities in the acetonitrile subphase, NPL dispersion or Teflon well setup. To reduce the impact of such external influences, experiments were conducted in the same environment and CdSe NPLs from the same synthesis batch and solvents from the same manifacturer and production batch were used where possible. Still, different self-assembly behavior of CdSe NPLs was observed in experiments from time to time and the underlying causes could not always be completely identified. Hence, additional measures like regulation of air flow and humidity should be considered in future self-assembly experiments.

# 4. Conclusion

In summary, the aim of this work was to develop a reliable procedure for the preparation of large, coherent monolayer and double layer films of CdSe NPLs with homogeneous surface coverage and collective orientation of nanoplatelets.

First, monolayer films were successfully prepared in self-assembly experiments of CdSe NPLs at the liquid interface. In these experiments, film formation resulted from solvent evaporation of nanoplatelet dispersions whereby the collective orientation of nanoplatelets was kinetically controlled by the choice of solvent. Three different methods of film deposition onto solid substrates were evaluated and optimized. Horizontal deposition according to method I and method II produced even, coherent monolayer films of uniformly oriented CdSe NPLs, either edge-up or face-down, and a size of 500-2000 $\mu m^2$. In method I, the substrate, a TEM grid, is placed on a level platform in the Teflon well and the final CdSe NPL film at the acetonitrile/air interface is slowly deposited by draining the acetonitrile subphase *via* a syringe. In method II, a TEM grid is lowered into the subphase after self-assembly of CdSe NPLs and film formation and carefully lifted again to deposit the monolayer of nanoplatelets onto the substrate. A third method, similar to dip-coating, yielded films of a similar size but did not maintain the collective orientation of face-down assembled nanoplatelets and thus resulted in a mixture of face-down and edge-up oriented CdSe NPLs. Hypotheses regarding this issue were developed and discussed, including fluctuations in solvent evaporation rates and a too fast and inconsistent deposition rate. However, self-assembly experiments in a covered Langmuir-Blodgett trough with controllable rate of the deposition process refuted both assumptions. It was suggested that nanoplatelets rearrange during vertical deposition onto a solid substrate, thus making a horizontal deposition better suited to the preparation of CdSe NPL monolayer films.

However, the optimized procedure for monolayer film preparation by self-assembly of nanoplatelets at the liquid interface, followed by vertical film deposition by method II was successfully transferred to the larger scale of the Langmuir-Blodgett setup, thus potentially enabling the coating of various larger substrates. Furthermore, compression isotherms of monolayer films were recorded to study the compression behavior of CdSe NPL monolayers. First experiments indicate that a non-reversible change of NPL orientation from face-down to edge-up can be evoked by horizontal compression of homogeneous films at the liquid interface, even though the obtained films still contained a certain fraction of face-down oriented NPLs. However, with further improvements, monolayer films with a uniform edge-up configuration of nanoplatetelets should also be accessible by the compressing method.

Having successfully developed a procedure for the preparation of large, coherent monolayer films of uniformly oriented CdSe NPLs, double-layer films of nanoplatelets were obtained by sequential horizontal deposition of a second monolayer on top of a first monolayer. Double layers of edge-up/edge-up, edge-up/face down and vice versa oriented nanoplatelets were prepared in this manner. Yet, obtaining face-down/face-down double layer films proved more challenging as many CdSe NPLs in the top layer seemed to rearrange into the edge-up orientation during deposition. Repulsive interactions between the dense ligand shells on wide facets of nanoplatelets in the upper and lower monolayer were suggested as an underlying cause. This hypothesis was tested by stripping ligands off the first CdSe NPL monolayer by treatment with short-chain alcohols. Treatment with methanol or ethanol allowed for the controlled deposition of a second face-down layer on top of a first face-down layer, yielding double layer films of up to 100 $\mu m^2$ in size. Still, results were hard to reproduce.

This could be caused by, *e.g.* impurities that could modulate the kinetics of the self-assembly process which govern controlled face-down deposition. For future work, film deposition by Langmuir-Schäfer method should be considered as it can be carried out in the same Langmuir trough and represents a promising technique for horizontal film deposition of CdSe NPL films which enables more controlled, automated film deposition onto various solid substrates with adjustable deposition rate.

# 5. Experimental section

## 5.1 Chemicals

Cadmium oxide (≥99.99), myristic acid (≥98%), oleic acid (90%) and ethanol (99.8%) were purchased from *Sigma Aldrich*. Selenium powder (99.999) and trifluoroacetic anhydride (99+%) were purchased from *Alfa Aesar*. $Cd(acetate)_2 \cdot 2\ H_2O$ (98%) and 1-octadecene (90%) were purchased from *Acros*. Trifluoroacetic acid (99%) and methyl acetate (≥99%) were purchased from *Merck*. Triethylamine (99.5%) and 2-propanol (≥99.5%) were purchased from *Fluka*. Methanol (≥99.8 %) was purchased from *VWR Chemicals*. Acetonitrile (99.9%) and n-hexane (≥95%) were purchased from *Fisher Scientific* and n-octane (≥99%) was purchased from *Roth*. All chemicals were used as received without any further purification steps.

## 5.2 Synthesis procedures

### 5.2.1 Synthesis of $Cd(myristate)_2$

Cadmium myristate was synthesized according to a procedure by ROSSINELLI *et al*.[63] In a 100 mL round-bottom flask, CdO (5.75 g, 44.78 mmol) and acetonitrile (20 mL) were mixed and stirred at room temperature (650 rpm). To this red suspension, trifluoroacetic acid (0.7 mL, 9.15 mmol) and trifluoroacetic anhydride (6.2 mL, 43.98 mmol) were added slowly with a syringe and the mixture was stirred for 10-15 more minutes. The now colorless reaction mixture was then heated up to 50 °C under stirring for 1 h. Meanwhile, myristic acid (10.23 g, 44.80 mmol), triethylamine (14 mL, 100.44 mmol) and 2-propanol (100 mL) were combined in a 500 mL Erlenmeyer flask and stirred until fully dissolved and a clear solution was obtained. Next, the cadmium trifluoroacetate solution was added dropwise to the 500 mL Erlenmeyer flask under constant stirring, resulting in an increasingly viscous reaction mixture. Halfway through, more 2-propanol (100 mL) was added. The colorless precipitate was vacuum-filtered, washed four times with cold methanol (50 mL) and dried in a vacuum oven at 45°C overnight. Two days later, the solid product was washed five more times with cold methanol (50 mL), vacuum-filtered and dried in a vacuum oven at 45°C overnight to obtain the final product.

### 5.2.2 Synthesis of CdSe nanoplatelets

The synthesis of 4 monolayer thick CdSe NPLs follows a procedure described by ROSSINELLI *et al.*[63] with slight modifications. In a 100 mL three-neck round-bottom flask, $Cd(myristate)_2$ (170.4 mg, 0.30 mmol) and selenium powder (12.0 mg, 0.15 mmol) were suspended in 1-octadecene (15 mL). The reaction mixture was heated up to 100 °C within 10 minutes and degassed under vacuum at 100°C for 13 minutes, giving a colorless to slightly yellowish solution. Under argon atmosphere, this solution was heated up further to 240 °C within 16 minutes. $Cd(acetate)_2 \cdot 2\ H_2O$ (80.0 mg, 0.35 mmol) was added quickly to the bright yellow reaction mixture at 188 °C, leading to a gradual color change from yellow to orange and finally dark red which marks the proceeding growth of nanocrystals. After keeping the temperature at 240 °C for 6 more minutes, the mixture was immediately cooled down to 200 °C using an air gun and then placed in a water bath at room temperature.

Oleic acid (0.5 mL) was added when the temperature reached 185°C and 5 mL n-hexane were transferred to the three-neck round-bottom flask once the dispersion had cooled down to room temperature. To separate the CdSe NPLs of different thicknesses and QDs, the mixture was centrifuged at 8000 rpm for 9 minutes. The orange supernatant, containing 5 ML CdSe NPLs and few CdSe QDs, was decanted whereas the precipitate, containing both 4 ML and 3 ML CdSe NPLs, was redispersed in 5 mL n-hexane and centrifuged again at 8000 rpm for 7 minutes. The yellow supernatant, containing 4 ML CdSe NPLs, was collected and stored at room temperature until remaining 3 ML NPLs precipitated from the n-hexane dispersion, approximately within 1-2 weeks. Then, agglomerated 3 ML CdSe NPLs were removed by centrifugation at 8000 rpm for 5 minutes. 4 ML CdSe NPLs in the supernatant were precipitated to remove remaining 1-octadecene by adding 5 mL of methyl acetate and storing the dispersion in a fridge at 5 °C for 4 hours. After another centrifugation step at 8000 rpm for 5 minutes, the precipitate of 4 ML CdSe NPLs was collected, redispersed in 5 mL n-hexane and then stored at room temperature.

### 5.2.3 Upscaled synthesis of CdSe nanoplatelets

4 ML CdSe NPLs were also synthesized by following an upscaled synthesis procedure described by ROSSINELLI *et al.*[64] First, Cd(myristate)$_2$ (680.4 mg, 1.20 mmol), selenium powder (48.2 mg, 0.60 mmol) and 1-octadecene (60 mL) were added to a 100 mL three-neck round-bottom flask. The reaction mixture was degassed under vacuum at room temperature for 30 minutes and then heated up to 240°C under argon atmosphere. At 200°C, Cd(acetate)$_2 \cdot 2$ $H_2O$ (256.0 mg, 0.96 mmol) was added quickly to the bright yellow solution. The mixture was kept at 240 °C for 8-9 more minutes before an air gun was used to cool down the reaction flask to 200°C. The flask was then placed in a water bath and allowed to cool to room temperature, oleic acid (3 mL) was added as soon as the temperature reached 185°C. Next, 10 mL n-hexane were added to the three-neck round-bottom flask and the reaction mixture was centrifuged at 8000 rpm for 10 minutes. The orange supernatant was decanted whereas the precipitate, containing both 4 ML and 3 ML CdSe NPLs, was redispersed in 20 mL n-hexane and left undisturbed for 1 hour to allow 3 ML CdSe NPLs to precipitate. The dispersion was then centrifuged again at 8000 rpm for 10 minutes and most agglomerated 3 ML CdSe NPLs were removed as the precipitate. After storing the yellow supernatant with 4 ML CdSe NPLs for 1-2 weeks at room temperature, this centrifugation step was repeated to remove residual 3 ML CdSe NPLs. The 4 ML CdSe NPL in the supernatant were precipitated by adding 20 mL of methyl acetate, followed up by storage in a fridge at 5°C for 4 hours and a last centrifugation step at 8000 rpm for 10 minutes. The precipitate of 4 ML CdSe NPLs was collected, redispersed in 20 mL n-hexane and stored at room temperature.

## 5.3. Self-assembly experiments

For self-assembly experiments, 4 ML CdSe NPLs were dispersed in either hexane or octane. To this end, aliquots of the CdSe NPL stock dispersion in hexane were taken and the solvent was removed *in vacuo* using a rotary evaporator. Then, CdSe NPLs were redispersed in the respective solvent and diluted to concentrations of $2.0 \cdot 10^{-8}$ mol/L - $4.0 \cdot 10^{-8}$ mol/L, which were verified by UV-Vis absorption spectroscopy using published extinction coefficients and the LAMBERT-BEER law.[26] The concentrations of diluted CdSe NPL samples which were used in self-assembly experiments are listed in Table 3. Self-assembly experiments were carried out at 20 °C.

*Table 3: Concentrations of CdSe NPL dispersions used in self-assembly experiments. Concentrations were determined by UV-Vis absorption spectroscopy.*

| sample | continuous phase | $c_{4ML}$ / $10^{-8}$ mol·L$^{-1}$ | synthesis batch |
|---|---|---|---|
| NiH007-H-1 | hexane | 2.98 | NiH007 |
| NiH007-H-2 | hexane | 3.52 | NiH007 |
| NiH007-O | octane | 3.56 | NiH007 |
| NiH007-LB-H | hexane | 3.58 | NiH007 |
| NiH007-LB-O | octane | 3.42 | NiH007 |
| RM401 | hexane | 3.60 | RM397 |

### 5.3.1 Self-assembly of CdSe nanoplatelets by method I

This method for the self-assembly of CdSe NPLs at the liquid interface was adapted from GAO *et al.*[4] and uses a Teflon well of 3.5 cm x 3.5 cm x 3 cm with a cylindrical hole of 1.5 cm diameter in the center, as is shown in Figure 7. A cylindrical Teflon post was positioned inside the well and served as a platform for the substrate on which the films were later transferred to. Different platforms were used, varying in the tilt of their flat surface from 0° to 10° and 20°. A hole near the bottom of one side of the well was plugged with a syringe in a small rubber plug which allowed for the slow removal of the subphase. First, 2.5 mL acetonitrile were added to the Teflon well as the lower liquid phase and the substrate, a carbon-coated copper TEM grid (PLANO, S160-4), was placed on the plateau. Then, 50 or 60 µL of the respective CdSe NPL dispersion in hexane or octane (NiH007-H-1, NiH007-H-2, NiH007-O) were added on top of the subphase. The Teflon well was covered with a glass dish to decelerate the evaporation of the alkane solvent for 40 minutes before the glass dish was removed. The remaining solvent of the CdSe NPL dispersion was given 20 additional minutes for complete evaporation. Eventually, the acetonitrile subphase was slowly drained using the syringe thus depositing the assembled film of CdSe NPLs on the substrate. During the enture procedure, the Teflon well was placed below a UV lamp (λ = 366 nm) for better observation of the film formation and transfer onto the substrate by the green fluorescence of CdSe NPLs.

### 5.3.2 Self-assembly of CdSe nanoplatelets by method II

2.5 mL acetonitrile were added to a Teflon well plugged with a syringe in a rubber plug but without a platform positioned in the center. Then, 50 or 60 µL of the CdSe NPL dispersion (NiH007-H-1, NiH007-H-2) were added on top and the Teflon well was covered with a glass dish to decelerate the evaporation of the alkane solvent. After 40 minutes, the glass dish was removed to allow for complete evaporation of the alkane solvent. After 20 minutes, the substrate, a carbon-coated copper TEM grid (PLANO, S160-4), was carefully lowered into the acetonitrile layer using a pair of tweezers. It is then removed again in an upward motion, thereby depositing the CdSe NPL film onto the substrate surface. During the whole procedure, the Teflon well was placed below a UV lamp (λ = 366 nm) for better observation of the film formation and transfer onto the substrate by the green fluorescence of CdSe NPLs

### 5.3.3 Self-assembly of CdSe nanoplatelets by method III

2.5 mL acetonitrile were added to a Teflon well plugged with a syringe in a rubber plug and the entire substrate, a carbon-coated copper TEM grid (PLANO, S160-4), was vertically dipped into the acetonitrile with a pair of tweezers hanging from a stand. Next, 50 or 60 µL of the CdSe NPL dispersion (RM401) were added on top of the subphase. After 60 minutes, the acetonitrile was slowly drained using the syringe to deposit the assembled film of CdSe NPLs onto the substrate. During the whole procedure, the Teflon well was placed in close proximity to a UV lamp (*λ* = 366 nm) for better observation of the film formation and transfer onto the substrate by the green fluorescence of CdSe NPLs.

### 5.3.5 Langmuir-Blodgett self-assembly of CdSe nanoplatelets

A *Kibron MicroTrough XS* was used for the self-assembly of 4 ML CdSe NPLs. Prior to deposition, both the Langmuir-Blodgett trough and the two barriers were thoroughly cleaned with ethanol and petroleum ether and the wire probe for the surface tension measurement was cleaned by flaming with a butane torch. Acetonitrile was used as a subphase and added to the Langmuir-Blodgett trough. After configuration of the trough and calibration of the sensor, the subphase and probe were left to stabilize for approximately 5 minutes. Next, a dispersion of 4 ML CdSe NPLs in either hexane or octane (NiH007-LB-H, NiH007-LB-O) was slowly applied on top of the acetonitrile layer with a 1 mL glass syringe. The cover was placed over the Langmuir-Blodgett trough setup for 40 minutes to decelerate the evaporation of the alkane solvent. Then, the cover was removed to let any remaining alkane solvent of the CdSe NPL dispersion evaporate. After 20 more minutes, the compression was started at the slowest barrier translation rate of 1 mm/min. The assembled monolayer film of 4 ML CdSe NPLs was transferred to carbon-coated copper TEM grids (PLANO, S160-4) by carefully withdrawing the substrate from the acetonitrile subphase.

## 5.4 Characterization methods

### 5.4.1 Absorption and photoluminescence spectroscopy

60 µL of 4 ML CdSe NPL dispersed in n-hexane were transferred to a quartz glass cuvette (10 mm) and diluted with 3 mL n-hexane. Photoluminescence spectra were recorded using a *Prizmatix Silver* high power LED ($\lambda_{max}$ = 369 nm) for excitation and *Avantes SensLine AvaSpec*-HSC-TEC-EVO for data collection. Absorption spectra were recorded using an *AvaLight-DH-S-BAL* as a light source. For concentration measurements, 700 µL 4 ML CdSe dispersed in either n-hexane or n-octane were transferred to a quartz glass cuvette (10 mm) and absorption spectra were recorded using an *Agilent Technologies Cary 60 UV-Vis* spectrophotometer.

### 5.4.2 Transmission Electron Microscopy

TEM images of CdSe NPLs as well as monolayer and double layer films of CdSe NPLs were recorded on a *JEOL 1400* microscope at 120 kV acceleration voltage. The samples were deposited on carbon-coated copper grids (400 mesh, PLANO S160-4) either by drop casting or by the self-assembled film deposition methods described in chapter 5.3.

### 5.4.3 Thermogravimetric Analysis

Thermogravimetric analysis (TGA) was conducted on 10 mg samples of 4 ML CdSe NPL precipitate in a 40 µL alumina crucible and at a heating rate of 10 °C/min. TGA was performed in air with a *TGA/DSC3+* by *Mettler-Toledo*. A sample was prepared by repeatedly adding colloidal 4 ML CdSe NPLs in hexane to the alumina crucible and allowing the volatile solvent to evaporate. This step was repeated until approximately 10 mg of dry material was accumulated.

### 5.4.4 Nuclear Magnetic Resonance Spectroscopy

Liquid NMR measurements were performed in deuterated solvents with a *Bruker Avance* 300 MHz spectrometer. In case of the $Cd(myristate)_2$ precursor, 10 mg of the solid was dissolved in pyridine-$d_5$ for characterization. For the analysis of 4 ML CdSe NPLs, the hexane solvent was removed from 200 µL of the stock dispersion *in vacuo* and the yellow residue was re-dispersed in deuterated chloroform for characterization. All $^1$H-NMR spectra were analyzed using the software *MestReNova* Version 14.1 from *Mestrelab Research S.L.*

# References


[1] W. Buhro, V. Colvin **2003**, *2*, 138–139.

[2] S. Ithurria, B. Dubertret **2008**, *130*, 16504–16505.

[3] S. Jana, T. Phan, C. Bouet *et al.* **2015**, *31*, 10532–10539.

[4] Y. Gao, M. Weidman, W. Tisdale **2017**, *17*, 3837–3843.

[5] B. Abécassis **2016**, *17*, 618–631.

[6] K. Miszta, J. de Graaf, G. Bertoni *et al.* **2011**, *10*, 872–876.

[7] C. Rowland, I. Fedin, H. Zhang *et al.* **2015**, *14*, 484–489.

[8] Z. Chen, B. Nadal, B. Mahler *et al. Adv. Funct. Mater.* **2014**, *24*, 295–302.

[9] J. Grim, S. Christodoulou, F. Di Stasio *et al.* **2014**, *9*, 891–895.

[10] W. Brütting, J. Frischeisen, T. Schmidt *et al. Phys. Status Solidi A* **2013**, *210*, 44–65.

[11] B. Abécassis, M. Tessier, P. Davidson *et al.* **2014**, *14*, 710–715.

[12] A. Antanovich, A. Prudnikau, A. Matsukovich *et al. J. Phys. Chem. C* **2016**, *120*, 5764–5775.

[13] M. Fox. *Optical properties of solids*. Oxford Univ. Press: Oxford, **2011**.

[14] S. Perrault. *Gold Nanoparticles for Efficient Tumour Targeting,* University of Toronto, **2010**.

[15] F. Rabouw, C. de Mello Donega **2016**, *374*, 58.

[16] T. Edvinsson **2018**, *5*, 180387.

[17] S. Ithurria, M. Tessier, B. Mahler *et al.* **2011**, *10*, 936–941.

[18] J. de Roo, M. Ibáñez, P. Geiregat *et al.* **2016**, *10*, 2071–2081.

[19] N. Anderson, M. Hendricks, J. Choi *et al.* **2013**, *135*, 18536–18548.

[20] J. Owen **2015**, *347*, 615–616.

[21] B. Abécassis. *Self-Assembly of Semiconducting Nanoplatelets,* Université Paris, **2016**.

[22] M. Olutas, B. Guzelturk, Y. Kelestemur *et al.* **2015**, *9*, 5041–5050.

[23] M. Nasilowski, B. Mahler, E. Lhuillier *et al.* **2016**, *116*, 10934–10982.

[24] B. Guzelturk, M. Olutas, S. Delikanli *et al.* **2015**, *7*, 2545–2551.

[25] C. She, I. Fedin, D. Dolzhnikov *et al.* **2014**, *14*, 2772–2777.

[26] A. Yeltik, S. Delikanli, M. Olutas *et al. J. Phys. Chem. C* **2015**, *119*, 26768–26775.

[27] R. Scott, J. Heckmann, A. Prudnikau *et al.* **2017**, *12*, 1155–1160.

[28] S. Glotzer, M. Solomon **2007**, *6*, 557–562.

[29] Z. Nie, A. Petukhova, E. Kumacheva **2010**, *5*, 15–25.

[30] M. Shim, P. Guyot-Sionnest **1999**, *111*, 6955–6964.

[31] I. Dozov, C. Goldmann, P. Davidson. *Permanent Dipoles in CdSe Nanoplatelets*, **2019**.

[32] G. Lauth, J. Kowalczyk. *Physik u. Chemie der Kolloide*. Springer Spektrum: Berlin, **2016**.

[33] D. Walker, B. Kowalczyk, M. de La Cruz *et al.* **2011**, *3*, 1316–1344.

[34] B. Fritzinger, R. Capek, K. Lambert *et al. J. Am. Chem. Soc.* **2010**, *132*, 10195–10201.

[35] F. Hesselink, A. Vrij, J. Overbeek. *J. Phys. Chem.* **1971**, *75*, 2094–2103.

[36] T. Tadros. *Polym J* **1991**, *23*, 683–696.

[37] A. Widmer-Cooper, P. Geissler **2014**, *14*, 57–65.

[38] A. Widmer-Cooper, P. Geissler **2016**, *10*, 1877–1887.

[39] R. Momper, H. Zhang, S. Chen *et al. Nano Lett.* **2020**, DOI 10.1021/acs.nanolett.9b05270.

[40] K. Seshan. *Handbook of thin-film deposition techniques*. Noyes Publ: Norwich, NY, **2002**.

[41] J. Crowell **2003**, *21*, S88-S95.

[42] D. Lee, M. Rubner, R. Cohen **2006**, *6*, 2305–2312.

[43] A. Gole, N. Jana, S. Selvan *et al.* **2008**, *24*, 8181–8186.

[44] K. Blodgett. *J. Am. Chem. Soc.* **1935**, *57*, 1007–1022.

[45] V. Vadim. *Langmuir–Blodgett method*. http://eng.thesaurus.rusnano.com/wiki/article1797.

[46] J. Zasadzinski, R. Viswanathan, L. Madsen *et al.* **1994**, *263*, 1726–1733.

[47] S. Paul, C. Pearson, A. Molloy *et al. Nano Lett.* **2003**, *3*, 533–536.

[48] H. Kaur, S. Yadav, A. Srivastava *et al.* **2016**, *6*, 34095.

[49] J. Puetz, M. Aegerter. *Dip Coating Technique*; Springer US: Boston, MA, **2004**.

[50] F. Ott, A. Riedinger, D. Ochsenbein *et al. Nano Lett.* **2017**, *17*, 6870–6877.

[51] A. Chakrabarty, S. Chatterjee, U. Maitra. *J. Mater. Chem. C* **2013**, *1*, 2136.

[52] J. Zemann. *Acta Cryst* **1965**, *18*, 139.

[53] C. Hartley, J. Dempsey. *Nano Lett.* **2019**, *19*, 1151–1157.

[54] B. Yang, J. Sharp, M. Smith **2016**, *6*, 32296.

[55] C. Tanford. *J. Phys. Chem.* **1972**, *76*, 3020–3024.

[56] E. Rio, F. Boulogne **2017**, *247*, 100–114.

[57] K. Lambert, R. Capek, M. Bodnarchuk *et al.* **2010**, *26*, 7732–7736.

[58] M. Tessier, L. Biadala, C. Bouet *et al.* **2013**, *7*, 3332–3340.

[59] B. Guzelturk, O. Erdem, M. Olutas *et al.* **2014**, *8*, 12524–12533.

[60] A. Hassinen, I. Moreels, K. de Nolf *et al. J. Am. Chem. Soc.* **2012**, *134*, 20705–20712.

[61] J. Song, H. Choi, Y.-H. Kim *et al. Adv. Energy Mater.* **2017**, *7*, 1700301.

[62] R. Knauf, J. Lennox, J. Dempsey. *Chem. Mater.* **2016**, *28*, 4762–4770.

[63] A. Rossinelli, A. Riedinger, P. Marqués-Gallego *et al.* **2017**, *53*, 9938–9941.

[64] A. Rossinelli, H. Rojo, A. Mule *et al. Chem. Mater.* **2019**, *31*, 9567–9578.

# List of figures

# List of tables

# Appendix

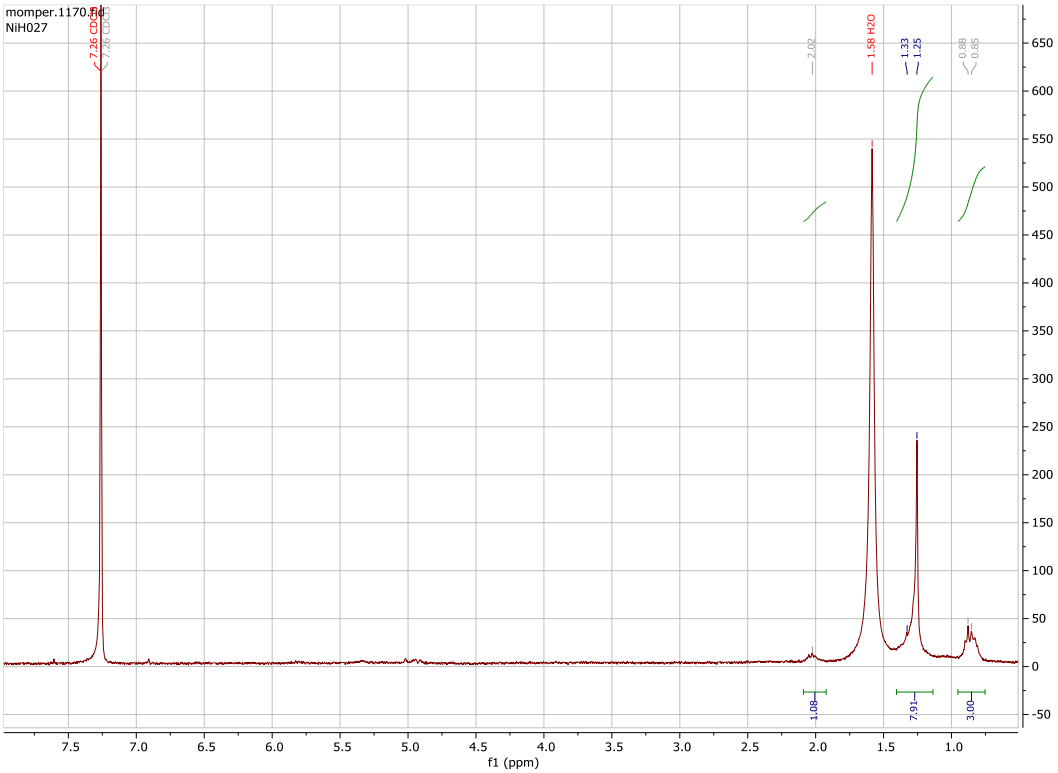


*Appendix 1: $^{1}$H-NMR of purified 4 ML CdSe NPLs measured in $CDCl_3$. No peaks associated with the double bond in oleic acid are present.*

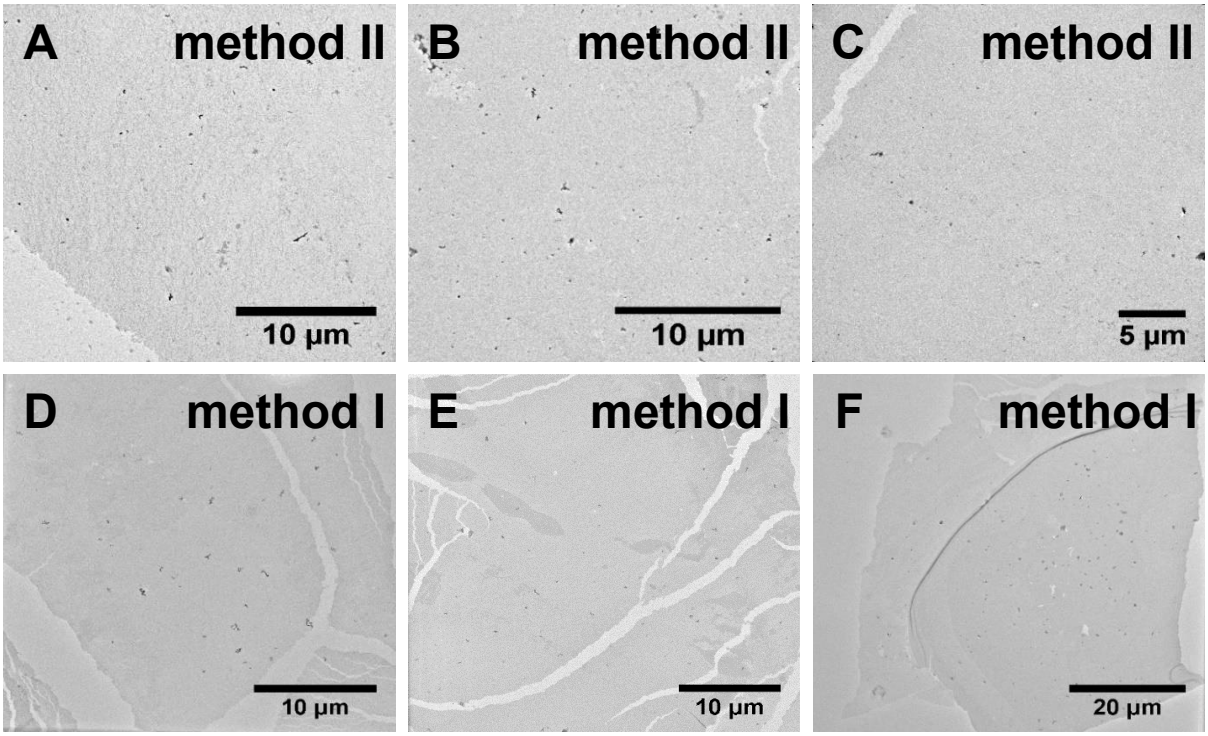


*Appendix 2: Low magnification TEM images of CdSe NPL monolayer films prepared by **method I** and **method II** on carbon-coated copper grids (A-C) and on silicium nitride grids (D-F).*

# Acknowledgements

First, I would like to thank Prof. Dr. Katharina Landfester for admitting me to the group and giving me the opportunity me to write my master thesis in this department.
I give specials thanks to my project leader Dr. Andreas Riedinger for his excellent supervision at all times during the six months of working on my master thesis and his detailed insights into the research field of semiconducting nanoplatelets.
I would also like to acknowledge Prof. Carsten Sönnichsen as the second reader of this master thesis.
Additionally, I'm very thankful for the support of Rebecca Momper who trained me in the synthesis of CdSe nanoplatelets and taught me about the self-assembly of CdSe nanoplatelets at the liquid interface. Thank you for the helpful insights and ideas, sharing your experience with self-assembly experiments helped me immensely in advancing with my project.
Of course I would also like to thank all the other members of the Riedinger group for the warm welcome, the fruitful discussions concerning this project and for any help with general concerns in the institute. Thank you as well for the pleasant working atmosphere, delightful entertainment and delicious snacks during our weekly group meetings.
Besides, I also give thanks to Yinzhou Guo for giving me an introduction to the Langmuir-Blodgett method and to Petra Räder for conducting Thermogravimetric Analysis on some of my samples.
Lastly, many thanks to my family and my friends for their unfailing support and continuous encouragement both throughout the years of my chemistry studies and through the process of researching and writing this master thesis. I'm deeply grateful that you always had my back and for cheering me up me when needed. Thank you!